directly related to cerebellar ataxia. However, HCV reactivation after LDLT may be, at least in part, a triggering factor for the neurological deficient in this case as discussed previously.[14]

In conclusion, we have proposed that cerebellar ataxia without other neurological findings is a new adverse event associated with calcineurin inhibitors. This condition was shown not to involve leukoencephalopathy using MRI. Ataxia caused a significant negative impact on the daily life of our patient. Reduction of the calcineurin inhibitor dose reversed her condition, but the change from Tac to CsA was not effective. Hence, it is important to determine whether neurologically adverse effects in transplanted patients originate from calcineurin inhibitors, and familiarity with the side effects of calcineurin inhibitors is important when using these agents.

REFERENCES

1. Bechstein WO: Neurotoxicity of calcineurin inhibitors: impact and clinical management. Transpl Int 13:313, 2000

2. Compston JE: Osteoporosis after liver transplantation. Liver Transpl 9:321, 2003

3. Stein DP, Lederman RJ, Vogt DP, et al: Neurological complications following liver transplantation. Ann Neurol 31:644, 1992

4. Sheth TN, Ichise M, Kucharczyk W: Brain perfusion imaging in asymptomatic patients receiving cyclosporin. Am J Neuroradiol 20:853, 1999

5. Vogt DP, Lederman RJ, Carey WD, et al: Neurologic complications of liver transplantation. Transplantation 45:1057, 1988

6. Sokol DK, Molleston JP, Filo RS, et al: Tacrolimus (FK 506)-induced mutism after liver transplant. Pediatr Neurol 28:156, 2003

7. Bronster DJ, Boccagni P, O'Rourke M, et al: Loss of speech after orthotopic liver transplantation. Transpl Int 8:234, 1995

8. Garcia-Escrig M, Martinez J, Fernandez-Ponsati J, et al: Severe central nervous system toxicity after chronic treatment with cyclosporine. Clin Neuropharmacol 17:298, 1994

9. Hinchey J, Chaves C, Appignani B, et al: A reversible posterior leukoencephalopathy syndrome. N Engl J Med 334:494, 1996

10. Belli LS, De Carlis L, Romani F, et al: Dysarthria and cerebellar ataxia: late occurrence of severe neurotoxicity in a liver transplant recipient. Transpl Int 6:176, 1993

11. Nussbaum ES, Maxwell RE, Bitterman PB, et al: Cyclosporine A toxicity presenting with acute cerebellar edema and brainstem compression. Case report. J Neurosurg 82:1068, 1995

12. Sato M, Suzuki K, Yamazaki H, et al: A pivotal role of calcineurin signaling in development and maturation of postnatal cerebellar granule cells. Proc Natl Acad Sci USA 102:5874, 2005

13. Filippini D, Colombo F, Jann S, et al: Central nervous system involvement in patients with HCV-related cryoglobulinemia: literature review and a case report. Reumatismo 54:150, 2002

14. Belli LS, De Carlis L, Romani F, et al: Dysarthria and cerebellar ataxia: late occurrence of severe neurotoxicity in a liver transplant recipient. Transpl Int 6:176, 1993

X-linked inhibitor of apoptosis (XIAP) and XIAP-associated factor-1 expressions and their relationship to apoptosis in human hepatocellular carcinoma and non-cancerous liver tissues

RYOSUKE SAKEMI[1-3], HIROHISA YANO[1,3], SACHIKO OGASAWARA[1,3], JUN AKIBA[1,3], OSAMU NAKASHIMA[1,3], SUGURU FUKAHORI[1,3], MICHIO SATA[2,3] and MASAMICHI KOJIRO[1,3]

[1]Department of Pathology and [2]Division of Gastroenterology, Department of Medicine, Kurume University School of Medicine; [3]Research Center of Innovative Cancer Therapy of the 21st Century COE Program for Medical Science, Kurume University, Kurume, Fukuoka 830-0011, Japan

Received March 1, 2007; Accepted April 2, 2007

Abstract. The X-linked inhibitor of apoptosis (XIAP) belongs to the inhibitor of apoptosis (IAP) family, and the action of XIAP is inhibited by XIAP-associated factor-1 (XAF1). In the present study, XIAP and XAF1 protein expressions and their relationship to apoptosis were investigated in hepatocellular carcinoma (HCC). We examined immunohistochemical expressions of XIAP and XAF1, and the number of apoptotic HCC cells in surgically resected tissues of 24 HCCs, consisting of 7 well-, 10 moderately and 7 poorly differentiated HCCs. As a result, XIAP and XAF1 expressions were identified in the cytoplasm of non-neoplastic and neoplastic hepatocytes. In the 24 HCCs, XIAP expression was not different according to the histological grade of HCC. In contrast, XAF1 expression was significantly lower in poorly differentiated than that in well- or moderately differentiated HCCs ($P=0.001$), or XIAP expression in poorly differentiated HCC ($P<0.001$). Apoptotic HCC cell number was significantly lower in poorly differentiated than that in well- or moderately differentiated HCCs ($P<0.01$). A significant relationship was observed between XAF1 expression and apoptotic cell number in HCC tissues. In conclusion, the present findings suggest that significantly low XAF1 expression, but not XIAP expression, in poorly differentiated HCC may relate to resistance to apoptosis.

Introduction

Apoptosis is an active process of gene-directed cellular self-destruction and is observed in the sculpting of organs and tissues during embryonic development and the removal of old unnecessary cells for the maintenance of tissue homeostasis. Apoptosis is also observed in some pathological processes, such as in the elimination of tumor cells and virus-infected cells, and thereby contributes to the self-defense mechanisms. In the process of apoptosis, activation of the caspase family, especially caspase-3, plays an important role (1-3).

The inhibitor of apoptosis (IAP) family contains intrinsic cellular regulators of apoptosis and includes X-linked IAP (XIAP), c-IAP1, c-IAP2, NAIP, ML-IAP, ILP-2, survivin and Apollon (4). These proteins are characterized by the presence of one to 3 copies of a ~70-amino acid domain termed the baculoviral inhibitory repeat (BIR) at the amino terminus of the protein. The BIR domains have been shown to bind and inhibit caspase-3, -7, and -9 (4-6). Among the IAP family, XIAP protein contains 3 copies of the BIR domain and one RING domain at the extreme carboxyl terminus of the protein. *In vitro* kinetic studies have shown that XIAP is the most potent caspase inhibitor and suppressor of apoptosis in the IAP family (4,6). Various levels of XIAP mRNA and protein were expressed in human cancer cell lines (7,8), suggesting the involvement of XIAP in the apoptosis resistance mechanism of cancer cells.

The caspase-inhibiting activity of XIAP is negatively regulated by at least two XIAP-interacting proteins, XIAP-associated factor-1 (XAF1) (8,9) and Smac/DIABLO (10,11). XAF1, a 34-kDa zinc finger protein, was identified in a yeast two-hybrid screen based on its ability to bind XIAP and was found to antagonize the ability of XIAP to suppress caspase activity and cell death *in vitro* (6). XAF1, which resides in the nucleus, can effect a relocalization of XIAP from the cytoplasm to nucleus and neutralize XIAP's ability to inhibit apoptosis (9). Smac/DIABLO, which is localized in mitochondria, is released into cytoplasm and processed into an active form during mitochondria-induced apoptosis (10,11). The binding of active Smac/DIABLO to XIAP is proposed to destabilize the XIAP-caspase interaction by steric hindrance, resulting in disruption of the XIAP-caspase complex (12,13). XAF1 is ubiquitously expressed in normal tissues, but is present at very low or undetectable levels in many cancer cell lines (8,9). Byun *et al* (14) found that a substantial fraction of gastric cancer cell lines and tissues express no or extremely low levels

Correspondence to: Dr Hirohisa Yano, Department of Pathology, Kurume University School of Medicine, 67 Asahi-machi, Kurume, Fukuoka 830-0011, Japan
E-mail: hiroyano@med.kurume-u.ac.jp

Key words: apoptosis, hepatocellular carcinoma, XIAP-associated factor-1, X-linked inhibitor of apoptosis

of the XAF1 transcript, whereas Smac/DIABLO was normally expressed in all cancer specimens.

Hepatocellular carcinoma (HCC) often develops in patients with hepatitis B or C virus-related chronic hepatitis or liver cirrhosis. In non-HCC tissues, apoptosis of hepatocytes, showing chromatin condensation of the nuclei and eosinophilic change of the cytoplasm, is often observed, and the number of such apoptotic cells is in proportion to inflammatory activity. On the other hand, abnormalities in the expression of apoptosis-related molecules, and the resistance to various apoptosis-inducing stimuli have been reported in HCC (15,16). Except for the study of Shiraki *et al* (17) who examined XIAP expression in HCC tissues, there have been no comparative studies on XAF1 and XIAP expressions according to the histological grade, and no study to explore the relationship between the frequency of apoptosis and XAF1 or XIAP expression in human HCC tissues. These are addressed in the present study.

Materials and methods

Tissue samples. Immunohistochemical examination was performed on formalin-fixed, paraffin-embedded sections of cancerous and non-cancerous tissues obtained from 24 surgically resected HCCs at the Kurume University Hospital between 1989 and 2003. The 24 patients ranged from 50 to 84 years of age, and consisted of 18 males and 6 females. Two were serum hepatitis B surface antigen-positive, 19 were positive to the hepatitis C virus antibody, and the remaining 3 patients were not positive to either. The 24 cases did not receive preoperative anticancer therapies such as transcatheter arterial embolization (TAE) and percutaneous ethanol injection therapy. Among the 24 cases, seven had well-differentiated HCC, 10 had moderately differentiated HCC, and 7 had poorly differentiated HCC. The non-HCC tissues showed liver cirrhosis in ten cases and chronic hepatitis in 14. Informed consent was obtained from all patients included in the study.

Immunohistochemistry. Formalin-fixed, paraffin-embedded serial sections (4 μm) were mounted on 3-aminopropyltriethoxysilane-coated slides (Matsunami Glass Ind., Ltd., Osaka, Japan), and deparaffinized in xylene alcohol and graded alcohol. For XIAP immunostaining, the sections were soaked in 10 mmol/l of sodium citrate buffer (pH 6.9) and treated in a microwave for 30 min for antigen retrieval. XIAP and XAF1 expressions were immunohistochemically examined with mouse monoclonal anti-XIAP antibody (3.0 μg/ml, BD Biosciences, San Jose, CA) and rabbit polyclonal anti-XAF1 antibody (4 μg/ml, IMGENEX, San Diego, CA) as the primary antibodies, and using catalyzed signal-amplification system II (Code K1497, Dako, Ely, UK) according to the manufacturer's protocol. The sections for XIAP immunostaining were incubated with primary antibody for 60 min at room temperature after blocking endogenous biotin and peroxidase activities, and the sections for XAF1 were incubated overnight with primary antibodies at 4°C. Negative controls were prepared by replacing the primary antibody with normal mouse IgG or normal rabbit IgG. The peroxidase reaction was developed with the addition of 3,3-diaminobenzidine and H_2O_2 substrate solution. After counterstaining with hematoxylin, the slides were dehydrated, coverslipped, and observed under a microscope (Olympus BH-2, Olympus Optical, Tokyo, Japan).

Evaluation of immunohistochemical findings. The results of immunohistochemistry were evaluated according to the rate of staining and grading of expression by two pathologists (Y.S. and H.Y.). XIAP and XAF1 expressions in non-HCC tissues are relatively homogeneous and were used as an internal positive control. Regarding XIAP and XAF1, an expression score system was assigned on the basis of multiplying the rate of cells staining positive by the intensity of staining. The staining intensity was scored on a scale from 0 to 2 (0, HCC cells with no positive reactions; 0.5, HCC cells stained less intensely than hepatocytes; 1.0, HCC cells stained as intensely as hepatocytes; 2.0, HCC cells more intensely stained than hepatocytes). The final score was calculated as the sum of each staining intensity multiplied by the rate of the corresponding area. For example: if a HCC nodule shows 30% HCC cells stained less intensely than hepatocytes, 50% HCC cells stained as intensely as hepatocytes, and 20% HCC cells more intensely stained than hepatocytes, the score would be (0.3x0.5) + (0.5x1.0) + (0.2x2.0) = 1.05.

Assessment of number of apoptosic cells in HCC tissues. The number of cells showing the characteristics of apoptosis (e.g., cytoplasmic shrinkage, chromatin condensation and nuclear fragmentation) was counted in 14-25 0.25 mm^2-areas within HCC nodules stained with hematoxylin-eosin (HE).

Statistics. Group differences were obtained for the expression score of XIAP and XAF1, and apoptosis number with the Mann-Whitney test. The correlation between the number of apoptosic cells and the expression of XIAP or XAF1 was examined by Pearson's correlation coefficient. All statistical analyses were performed with StatMate III (ATMS Co., Ltd., Tokyo, Japan). P-values <0.05 were considered significant.

Results

XIAP and XAF1 expressions in HCC and non-HCC tissues. In non-HCC tissue, XIAP was expressed in the cytoplasm of hepatocytes, and the XIAP-expressing cells were relatively homogeneously distributed in the liver lobule (Fig. 1A and B). XAF1 was also expressed in the cytoplasm of hepatocytes. The XAF1-expressing cells were almost homogeneously distributed, but the more strongly expressing cells were scattered in the areas around portal tracts with marked cellular infiltration (Fig. 1C). Cirrhosis and chronic hepatis did not differ in the intensity or distribution of XAF1 expression. Negative controls showed no staining for XIAP or XAF1 (data not shown).

In HCC tissue, XIAP was expressed in the cytoplasm of HCC cells, and the XIAP-expressing cells in cancer nodules were more homogeneously distributed than the XAF1-expressing cells (Fig. 2A and B). XAF1 was also expressed in the cytoplasm of HCC cells. However, the XAF1 expression levels in well- and moderately differentiated HCC nodules varied with individual cancer cells, showing a heterogeneous distribution. In particular, XAF1 expression was conspicuous in HCC cells with fatty change and immediately subcapsular HCC cells in the periphery of cancer nodules (Fig. 2A and B; Fig. 3).

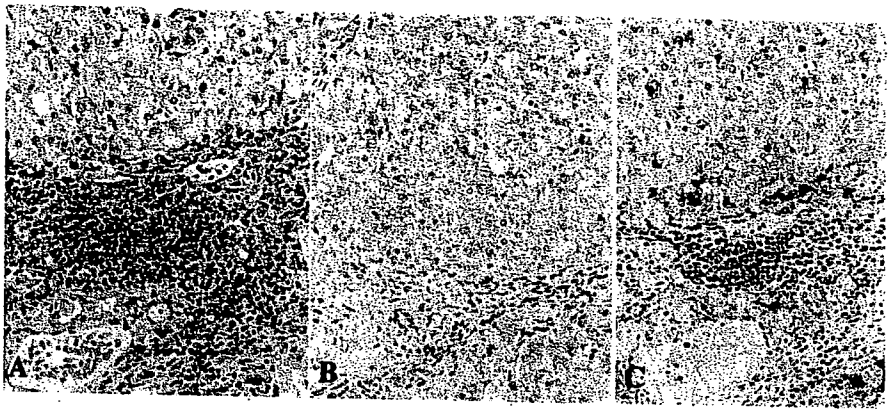

Figure 1. (A) Photomicrograph showing a portal area with active infiltration of lymphocytes, and periportal non-neoplastic hepatocytes (hematoxylin-eosin stain, x100). (B) Immunohistochemical staining for XIAP showing homogeneous expression in hepatocytes (counterstained with Mayer's hematoxylin, x100). (C) Immunohistochemical staining for XAF1 showing homogeneous expression in hepatocytes, except in those around the portal areas with active infiltration of inflammatory cells, which showed strong expression (counterstained with Mayer's hematoxylin, x100).

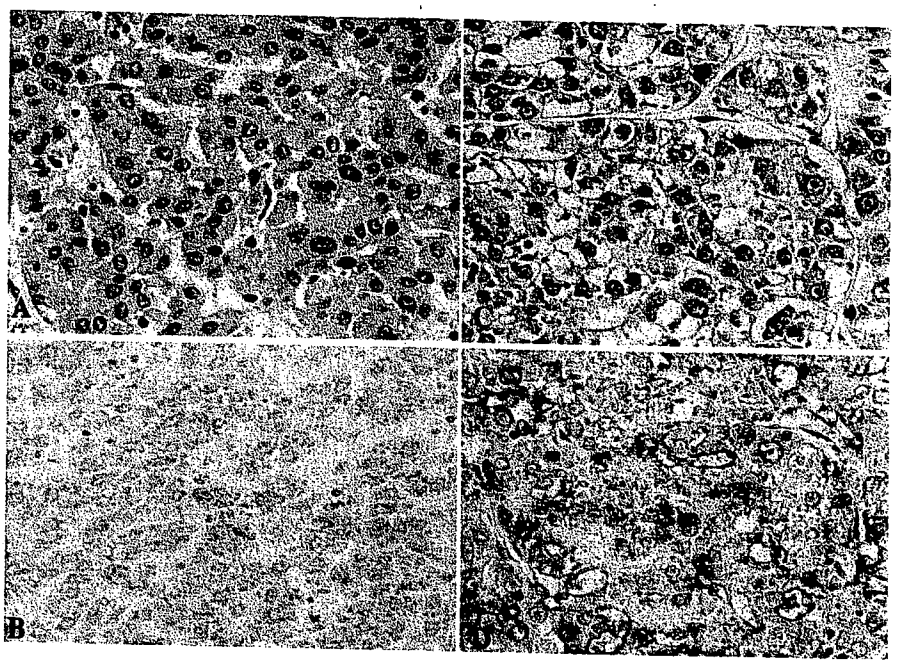

Figure 2. (A) Photomicrograph showing moderately differentiated hepatocellular carcinoma (HCC) with a thick trabecular arrangement (hematoxylin-eosin stain, x200). (B) Immunohistochemical staining for XIAP showing homogeneous expression in HCC cells (counterstained with Mayer's hematoxylin, x200). (C) Photomicrograph showing moderately differentiated HCC with fatty change and a relatively compact arrangement (hematoxylin-eosin stain, x200). (D) Immunohistochemical staining for XAF1 showing strong expression in HCC cells with fatty change (counterstained with Mayer's hematoxylin, x200).

The numbers of well-, moderately and poorly differentiated HCCs with an XIAP expression score of 1 or higher were 5 (71%), 5 (50%) and 6 (86%), respectively. The XIAP expression scores in the well-, moderately and poorly differentiated HCCs were 1.07±0.44 (mean ± SD), 1.10±0.69 and 1.17±0.38, respectively, showing no significant differentiation-dependent differences [Fig. 4 (left panel)]. The numbers of well-, moderately and poorly differentiated HCCs with an XAF1 expression score of 1 or higher were 6 (86%), 6 (60%) and 0 (0%), respectively. The XAF1 expression scores in the well-, moderately and poorly differentiated HCCs were 1.14±0.54 (mean ± SD), 1.14±0.47 and 0.19±0.16, respectively, indicating that the expression was significantly lower in the poorly differentiated HCCs than in the well- and moderately differentiated HCCs [P<0.001, Fig. 4 (left panel)]. In the poorly differentiated HCCs, the expression score of XAF1 was significantly lower than that of XIAP [P<0.001, Fig. 4 (right panel)]. No other differentiation-dependent differences were noted between the expression scores of XIAP and XAF1.

Presence of apoptosis and its relationship to XIAP and XAF1 expression in HCC. Fig. 5A shows typical apoptotic tumor cells (arrows) in moderately differentiated HCC tissue. The numbers of apoptotic cells per area in well-, moderately and poorly differentiated HCC nodules were 3.55±1.86 (mean ± SD), 3.62±1.46 and 1.76±0.46, respectively, indicating that the number of apoptotic cells was significantly smaller in the poorly differentiated than in the well- and moderately differentiated HCCs (P<0.01, Fig. 5B). In the 24 HCCs, the number of apoptotic cells per area was significantly correlated with XAF1 expression, but not with XIAP expression (Fig. 6).

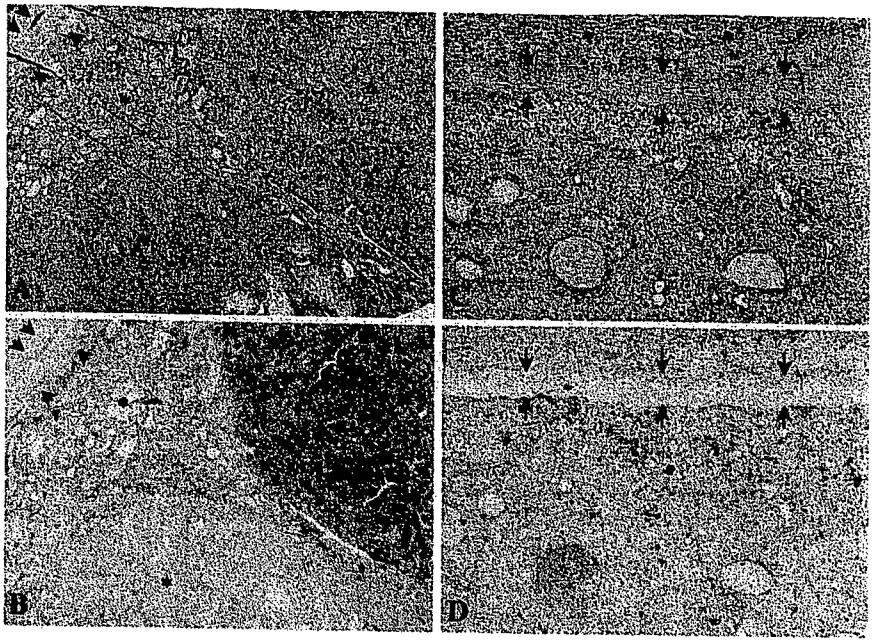

Figure 3. (A) Photomicrograph showing a hepatocellular carcinoma (HCC) nodule with a fibrous capsule (arrows). The nodule contains areas of moderately differentiated HCC with a trabecular arrangement (*), that with a pseudoglandular arrangement (•), and that with fatty change (Δ) (hematoxylin-eosin stain, x5). (B) Immunohistochemical staining for XAF1 showing heterogeneous expression. Upper right areas of moderately differentiated HCC with fatty change (Δ) and surrounding moderately differentiated HCC show strong expression, whereas the other areas show low levels of expression (counterstained with Mayer's hematoxylin, x5). (C) Photomicrograph showing a HCC nodule with a fibrous capsule (arrows) surrounded by non-HCC tissues (•) (hematoxylin-eosin stain, x20). (D) Immunohistochemical staining for XAF1 showing that HCC cells near the capsule (arrows) tend to show stronger XAF1 expression (counterstained with Mayer's hematoxylin, x20).

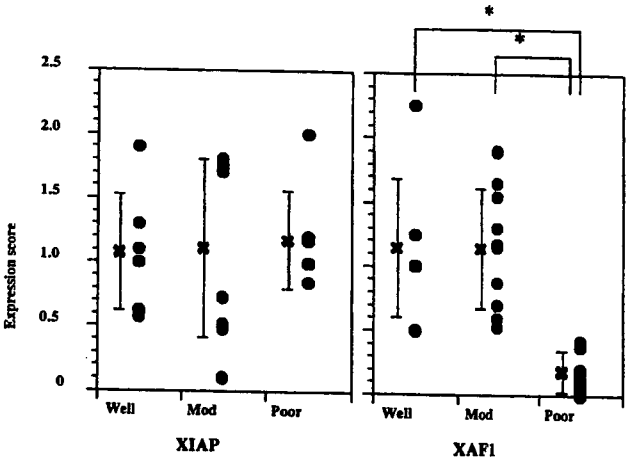

Figure 4. (Left panel) Expression scores of XIAP and XAF1 according to the histological grade of hepatocellular carcinoma (HCC). (Right panel) Comparison of expression scores between XIAP and XAF1 in poorly differentiated HCC. Data represent the mean ± SD (n=7-10). Well, well-differentiated HCC; mod, moderately differentiated HCC; poor, poorly differentiated HCC. *P<0.001 by the Mann-Whitney test.

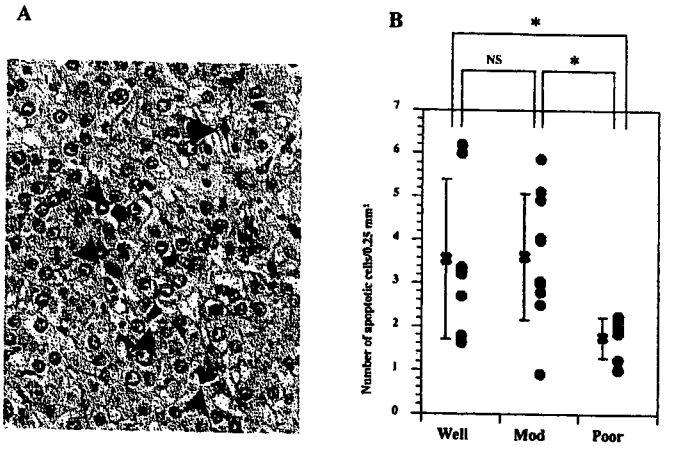

Figure 5. (A) Photomicrograph showing typical apoptotic tumor cells (arrows) with eosinophilic shrunken cytoplasm and pyknotic nuclei in moderately differentiated hepatocellular carcinoma (HCC) tissue (hematoxylin-eosin stain, x400). (B) Number of apoptotic HCC cells according to the histological grade. Data represent the mean ± SD (n=7-10). Well, well-differentiated HCC; mod, moderately differentiated HCC; poor, poorly differentiated HCC; NS, not significant. *P<0.01 by the Mann-Whitney U test.

Discussion

A recent immunohistochemical study revealed that the expression of XIAP protein in normal human tissues was heterogeneous and showed a higher selectivity to particular cell types (18). The expression of XIAP has also been confirmed in various tumor cell lines by Western blot analysis (7) and in various malignant neoplastic tissues, including non-small cell lung cancer, cervical carcinoma, prostate carcinoma and esophageal squamous cell carcinoma by immunohistochemistry, in which a higher expression was observed compared with normal counterparts (reviewed in ref. 18). These results suggest that overexpression of XIAP may contribute to resistance to apoptosis in various types of cancer cells. Studies using immunostaining have reported that XIAP protein is absent or weakly expressed in normal liver and the non-cancerous tissue of HCC (17,18). In contrast, Shiraki *et al* (17) reported that 14 of 20 (70%) HCC tissue samples demonstrated moderate or strong cytoplasmic staining for XIAP, and that XIAP expression was inversely correlated with apoptosis in

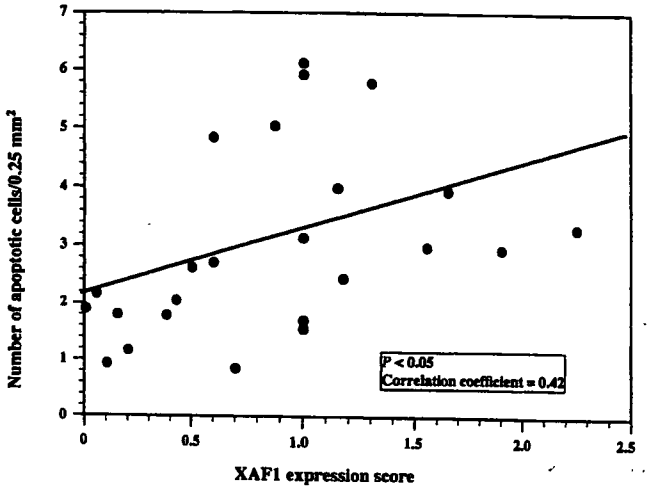

Figure 6. Relationship between the XAF1 expression score and the number of apoptotic tumor cells in hepatocellular carcinoma. Correlation of the coefficient rate is 0.42 ($P<0.05$).

HCC (17). In this study, HCC specimens with an XIAP expression score of 1 (indicating the same staining intensity in cancerous and non-cancerous tissues) or higher accounted for 16/24 (67%), about half of which showed moderate to marked expression, with no significant differentiation-dependent differences [Fig. 4 (left panel)] or relationship between XIAP expression and cancer cell apoptosis.

We examined immunohistochemically the XAF1 protein expression in human HCC tissues and non-HCC tissues. Previous studies revealed that XAF1 mRNA is expressed ubiquitously in all normal adult and fetal tissues including the liver (8,9). In non-HCC tissues, XAF1 was almost homogeneously expressed in non-neoplastic hepatocytes, except in those around the portal areas with active infiltration of inflammatory cells, which showed strong expression. Possible causes of this are: 1) The strong XAF1 expression could be mediated by inflammatory cytokines released from inflammatory cells, Leaman *et al* (19) found that XAF1 mRNA expression is upregulated by inflammatory cytokines, such as interferon (IFN)-γ and tumor necrosis factor-α. 2) Strong XAF1 expression in periportal hepatocytes may be related with the progression of cytotoxic T lymphocyte-induced apoptosis, probably via the Fas/Fas ligand system (16).

In contrast to the normal tissues, XAF1 is present at very low or undetectable levels in a variety of cancer cell lines (8,9), including melanoma (20), colorectal cancer (21), urinary bladder cancer, renal cancer and prostate cancer cell lines (22). In addition, XAF1 mRNA expression in melanoma tissues was significantly reduced compared with benign melanocytic nevi (20), and XAF1 mRNA in primary gastric tumors (14), and bladder transitional cell carcinoma and renal cell carcinoma tissues (22) were substantially lower compared with the non-cancerous tissue. Lee *et al* (22) found that hypermethylation at 14 CpG sites in the 5' proximal region of the XAF1 promoter was highly prevalent in cancers versus adjacent normal or benign tissue and tightly associated with reduced gene expression. Nodules of HCC, particularly well- and moderately differentiated HCCs, were characterized by the heterogeneous (areas of high and low) expression of XAF1, with a tendency toward high expression in HCC cells with fatty change and in the periphery of cancer nodules. On the other hand, XAF1 expression was lower in the poorly differentiated than in the well- and moderately differentiated HCCs. Abnormal reduction of XAF1 mRNA which showed a good correlation with tumor grade, was also reported in gastric and bladder carcinomas (14,22). We found a significant correlation between XAF1 expression and apoptosis; a significant reduction in apoptosis was observed in the poorly differentiated HCCs with a significantly lower expression of XAF1. It has been reported that the relative increase of XIAP to XAF1 expression may provide a survival advantage for tumor cells through the relative increase of XIAP antiapoptotic function (9). XAF1 inactivation in poorly differentiated HCC might contribute to the resistance to apoptosis and malignant progression of HCC. The causes of abnormal expression of XAF1 in HCC require further investigation.

Although this study immunohistochemically demonstrated the expression of XAF1 in the cytoplasm of neoplastic and non-neoplastic hepatocytes, endogenous XAF1 has been reported to be localized in the nucleus (8). However, XAF1 expression has been immunohistochemically detected in both the nucleus and cytoplasm of melanoma and benign nevus cells (20). In addition, its expression has also been noted in the cytoplasm and nucleus of XAF1-transfected 253J cells (22) and IFN-ß-stimulated A375 melanoma cells. Although it is not clear why XAF1 expression was demonstrable only in the cytoplasm in this study, we speculate that the causes of this are related to features specific to hepatocytes and the epitope accessibility of the antibody used. Therefore, further studies need to be performed using cell lines and different antibodies.

Type I IFN, including IFN-α and IFN-ß, has various biologic functions, such as an antiproliferative action (23,24). Recently, XAF1 was identified as an IFN-stimulated gene that contributes to IFN-dependent sensitization of cells to tumor necrosis factor-related apoptosis-inducing ligand-induced apoptosis (19). IFNs induced high levels of XAF1 protein predominantly in cell lines sensitive to the proapoptotic effects of IFN-ß (19). The direct antiproliferative effect of various type I IFN preparations and IFN-α subtypes on HCC cell lines has been reported (25-27) and upregulation of XAF1 mRNA following PEG-IFN-α2b treatment was also observed in the human HCC cell line HAK-1B (unpublished data). In clinical practice, IFN-α in combination with 5-fluorouracil (FU) has been used for the treatment of advanced HCCs, and the recent objective response rate of combination chemotherapy with IFN-α and 5-FU was 52% among HCC patients with portal venous invasion (28). We speculate that XAF1 could be related with the susceptibility to the therapy, and HCCs with the loss or low levels of XAF1 could be more resistant to the combination therapy than HCCs with normal XAF1 expression. Further study is required to examine whether or not XAF1 expression could be a clinically useful marker for the prediction of the outcome of combination chemotherapy with IFN-α and 5-FU.

Acknowledgements

We thank Ms. Sachiyo Maeda and Misato Shiraishi for their assistance in our experiments. This study was supported in

part by the Sarah Cousins Memorial Fund, Boston, MA, and by a Grant-in-Aid from the Ministry of Health, Labor and Welfare of Japan (No. 17200501).

References

1. Nagata S: Apoptosis by death factor. Cell 88: 355-365, 1997.
2. Vaux DL, Haecker G and Strasser A: An evolutionary perspective on apoptosis. Cell 76: 777-779, 1994.
3. Thompson CB: Apoptosis in the pathogenesis and treatment of disease. Science 267: 1456-1462, 1995.
4. Salvesen GS and Duckett CS: IAP proteins: blocking the road to death's door. Nat Rev Mol Cell Biol 3: 401-410, 2002.
5. Deveraux QL, Takahashi R, Salvesen GS and Reed JC: X-linked IAP is a direct inhibitor of cell-death proteases. Nature 388: 300-304, 1997.
6. Holcik M, Gibson H and Korneluk RG: XIAP: apoptotic brake and promising therapeutic target. Apoptosis 6: 253-261, 2001.
7. Tamm I, Kornblau SM, Segall H, *et al*: Expression and prognostic significance of IAP-family genes in human cancers and myeloid leukemias. Clin Cancer Res 6: 1796-1803, 2000.
8. Fong WG, Liston P, Rajcan-Separovic E, St Jean M, Craig C and Korneluk RG: Expression and genetic analysis of XIAP-associated factor 1 (XAF1) in cancer cell lines. Genomics 70: 113-122, 2000.
9. Liston P, Fong WG, Kelly NL, *et al*: Identification of XAF1 as an antagonist of XIAP anti-Caspase activity. Nat Cell Biol 3: 128-133, 2001.
10. Verhangen AM, Ekert PG, Pakusch M, *et al*: Identification of DIABLO, a mammalian protein that promotes apoptosis by binding to and antagonizing IAP proteins. Cell 102: 43-53, 2000.
11. Du C, Fang M, Li Y, Li L and Wang X: Smac, a mitochondrial protein that promotes cytochrome c-dependent caspase activation by eliminating IAP inhibition. Cell 102: 33-42, 2000.
12. Liu Z, Sun C, Olejniczak ET, *et al*: Structural basis for binding of Smac/DIABLO to the XIAP BIR3 domain. Nature 408: 1004-1008, 2000.
13. Wu G, Chai J, Suber TL, Wu JW, Du C, Wang X and Shi Y: Structural basis of IAP recognition by Smac/DIABLO. Nature 408: 1008-1012, 2000.
14. Byun DS, Cho K, Ryu BK, Lee MG, Kang MJ, Kim HR and Chi SG: Hypermethylation of XIAP-associated factor 1, a putative tumor suppressor gene from the 17p13.2 locus, in human gastric adenocarcinomas. Cancer Res 63: 7068-7075, 2003.
15. Yano H, Fukuda K, Haramaki M, Momosaki S, Ogasawara S, Higaki K and Kojiro M: Expression of Fas and anti-Fas-mediated apoptosis in human hepatocellular carcinoma cell lines. J Hepatol 25: 454-464, 1996.
16. Higaki K, Yano H and Kojiro M: Fas antigen expression and its relationship with apoptosis in human hepatocellular carcinoma and non-cancerous tissues. Am J Pathol 149: 429-437, 1996.
17. Shiraki K, Sugimoto K, Yamanaka Y, *et al*: Overexpression of X-linked inhibitor of apoptosis in human hepatocellular carcinoma. Int J Mol Med 12: 705-708, 2003.
18. Vischioni B, van der Valk P, Span SW, Kruyt FA, Rodriguez JA and Giaccone G: Expression and localization of inhibitor of apoptosis proteins in normal human tissues. Hum Pathol 37: 78-86, 2006.
19. Leaman DW, Chawla-Sarkar M, Vyas K, Reheman M, Tamai K, Toji S and Borden EC: Identification of X-linked inhibitor of apoptosis-associated factor-1 as an interferon-stimulated gene that augments TRAIL Apo2L-induced apoptosis. J Biol Chem 277: 28504-28511, 2002.
20. Ng KC, Campos EI, Martinka M and Li G: XAF1 expression is significantly reduced in human melanoma. J Invest Dermatol 123: 1127-1134, 2004.
21. Ma TL, Ni PH, Zhong J, Tan JH, Qiao MM and Jiang SH: Low expression of XIAP-associated factor 1 in human colorectal cancers. Chin J Dig Dis 6: 10-14, 2005.
22. Lee MG, Huh JS, Chung SK, *et al*: Promoter CpG hypermethylation and downregulation of XAF1 expression in human urogenital malignancies: implication for attenuated p53 response to apoptotic stresses. Oncogene 25: 5807-5822, 2006.
23. Pestka S, Langer JA, Zoon KC and Samuel CE: Interferons and their actions. Ann Rev Biochem 56: 727-777, 1987.
24. Gutterman JU: Cytokine therapeutics: lessons from interferon α. Proc Natl Acad Sci USA 91: 1198-1205, 1994.
25. Yano H, Yanai Y, Momosaki S, *et al*: Growth inhibitory effects of interferon-α subtypes vary according to human liver cancer cell lines. J Gastroenterol Hepatol 21: 1720-1725, 2006.
26. Yano H, Ogasawara S, Momosaki S, *et al*: Growth inhibitory effects of pegylated IFN α-2b on human liver cancer cells *in vitro* and *in vivo*. Liver Int 26: 964-975, 2006.
27. Yano H, Iemura A, Haramaki M, Ogasawara S, Takayama A, Akiba J and Kojiro M: Interferon alfa receptor expression and growth inhibition by interferon alfa in human liver cancer cell lines. Hepatology 29: 1708-1717, 1999.
28. Obi S, Yoshida H, Toune R, *et al*: Combination therapy of intraarterial 5-fluorouracil and systemic interferon-alpha for advanced hepatocellular carcinoma with portal venous invasion. Cancer 106: 1990-1997, 2006.

JOURNAL OF INTERFERON & CYTOKINE RESEARCH 27:507–516 (2007)

DOI: 10.1089/jir.2007.0183

Growth Inhibitory Effects of IFN-β on Human Liver Cancer Cells *In Vitro* and *In Vivo*

SACHIKO OGASAWARA, HIROHISA YANO, SEIYA MOMOSAKI, JUN AKIBA, NAOYO NISHIDA, SAKIKO KOJIRO, FUKUKO MORIYA, HIRONORI ISHIZAKI, KEITARO KURATOMI, and MASAMICHI KOJIRO

ABSTRACT

We investigated the effects of interferon-β (IFN-β) on the growth of human liver cancer cells. The effects of IFN-β with or without 5-fluorouracil (5-FU) on the proliferation of 13 liver cancer cell lines were investigated *in vitro*. Chronologic change in IFN-α receptor 2 (IFNAR-2) expression was monitored in hepatocellular carcinoma (HCC) cells (HAK-1B) cultured with IFN-β. After HAK-1B cells were transplanted into nude mice, various doses of IFN-β were administered, and the tumor volume, weight, histology, tumor blood vessel, and angiogenesis factor expression were examined. IFN-β inhibited the growth of 11 cell lines with apoptosis in a dose-dependent and time-dependent manner. With IFN-β, IFNAR-2 expression in HAK-1B cells was significantly downregulated from 6 to 12 h. IFN-β induced a dose-dependent decrease in tumor volume and weight and a significant increase of apoptosis in the tumor. Both basic fibroblast growth factor (bFGF) and blood vessel number in the tumor decreased only in mice receiving the lowest dose (1000 IU) of IFN-β. IFN-β with 10 μM of 5-FU frequently induced synergistic antiproliferative effects. IFN-β with or without 5-FU induces strong antitumor effects in HCC cells, and we conclude that IFN-β is useful for the prevention and treatment of HCC.

INTRODUCTION

INTERFERONS (IFNs) ARE A FAMILY of cytokines that possess various biologic activities, such as antiviral, antiproliferative, antiangiogenetic, immunomodulatory, and antitelomerase activities.[1–3] IFNs are classified into two major groups, type I IFN that includes IFN-α, IFN-β, and IFN-ω, and type II IFN, IFN-γ.[4] Both type I and type II IFNs bind with distinct cellular receptors and activate distinct and overlapping pathways.[5]

Hepatocellular carcinoma (HCC) is one of the most frequently found primary cancers, and many HCC patients have chronic hepatitis or cirrhosis caused by chronic infection with hepatitis B virus (HBV) or hepatitis C virus (HCV) as their background disease.[6–8] IFN-α and IFN-β have been used in the treatment of virus-related chronic hepatitis to eradicate these viruses. Recently, IFN-α and IFN-β have been shown to possess highly suppressive effects on hepatocellular carcinogenesis and on the recurrence of HCC after curative treatment in patients with virus-related chronic hepatitis.[9–13] The precise mechanisms of these suppressive actions have not yet been clarified, but direct antiproliferative effects of IFN-α and IFN-β may be involved. As IFN-α and IFN-β have various antitumor properties, they have been used in the treatment of such malignant diseases as melanoma, renal cell carcinoma (RCC), and chronic myelogeneous leukemia (CML).[14–16] Recent studies reported that administration of IFN-α in combination with chemotherapeutic agents, such as 5-fluorouracil (5-FU), was also effective against advanced HCC cases, including those showing tumor invasion into the major branches of the portal vein.[17–19]

Many researchers have investigated the antiproliferative effects and action mechanisms of IFN-α *in vitro* and *in vivo* by using liver cancer cell lines.[20–27] We have reported that (1) each IFN-α preparation or subtype presents very different antiproliferative activities in different human HCC cell lines, (2) a common mechanism of *in vitro* growth suppression by IFN-α is cell cycle arrest with or without caspase-dependent apoptosis induction, and (3) the mechanism of *in vivo* growth inhibi-

Department of Pathology, Kurume University School of Medicine, and Research Center of Innovative Cancer Therapy of the 21st Century COE Program for Medical Science, Kurume University, Kurume 830-0011, Japan.

tion by IFN-α is the induction of apoptosis with or without inhibition of angiogenesis.[20–24] However, IFN-β, another important IFN that is also used in treatment of chronic virus-related hepatitis, has not been investigated in as much detail as IFN-α, and there have been only a few basic *in vitro* studies published in the literature.[28–30] Therefore, its antitumor properties on HCC cells *in vitro* and *in vivo* remain to be clarified. In the current study, we investigated (1) the antiproliferative effects of IFN-β on liver cancer cell lines *in vitro* and *in vivo*, (2) chronologic changes in the expression of type I IFN receptor 2 (IFNAR-2) subunit and its relationship with antitumor effects on HCC cells treated with IFN-β, and (3) the antiproliferative effects of IFN-β alone or in combination with 5-FU on liver cancer cell lines *in vitro*.

MATERIALS AND METHODS

Cell lines and cell culture

This study used 11 HCC cell lines (KIM-1, KYN-1, KYN-2, KYN-3, HAK-1A, HAK-1B, HAK-2, HAK-3, HAK-4, HAK-5, and HAK-6) and 2 human combined hepatocellular and cholangiocarcinoma (CHC) cell lines (KMCH-1 and KMCH-2). These HCC and CHC cell lines were originally established in our laboratory, and each cell line retains the morphologic and functional features of the original tumor as described elsewhere.[31–39] The cells were grown in Dulbecco's modified Eagle's medium (DMEM) (Nissui Seiyaku, Tokyo, Japan) supplemented with 2.5% heat-inactivated (56°C, 30 min) fetal bovine serum (FBS) (Bioserum, Victoria, Australia), 100 U/mL penicillin, 100 μg/mL streptomycin (GIBCO-BRL/Life Technologies, Inc., Gaithersburg, MD), and 12 mmol/L sodium bicarbonate in a humidified atmosphere of 5% CO_2 in air at 37°C.

IFN and reagents

IFN-β (FERON) was kindly provided by Toray Industries (Tokyo, Japan), and the specific activity of IFN-β was 2×10^8 IU/mg protein. 5-FU was purchased from Kyowa Hakko Co. (Tokyo, Japan), fluorescein isothiocyanate-conjugated goat anti-mouse immunoglobulin (FITC-GAM) was from BD Biosciences (San Jose, CA), control normal mouse IgG1 was from DAKO (Glostrup, Denmark); rat antibody against mouse endothelial cells (anti-CD34, clone MEC14.7) was from Serotec Ltd. (Oxford, U.K.), mouse monoclonal antibody (mAb) against human α-smooth muscle actin (SMA) that cross-reacts with mouse α-SMA (clone 1A4) was from Immunon (Pittsburgh, PA), and mouse mAb against human IFNAR-2 was from Chemicon International (Temecula, CA).

Effects of IFN-β on proliferation of HCC and CHC cell lines in vitro

The effects of IFN-β on the growth of the cultured cells were examined with colorimetry using 3-(4,5-dimethylthiazol-2yl)-2,5-diphenyl tetrazolium bromide (MTT) assay kits (Chemicon) as described elsewhere.[20,24] Briefly, the cells ($1.5–6 \times 10^3$ cells/well) were seeded onto 96-well plates (Nunc, Roskilde, Denmark) and cultured for 24 h, and the culture medium was changed to new medium with or without IFN-β (16, 64, 256, 1024, or 4096 IU/mL). After culture for 24, 48, 72, or 96 h, the number of viable cells was examined.

Morphologic observation

For morphologic observation under a light microscope, cultured cells were seeded on Lab-Tek tissue culture chamber slides (Nunc), cultured with or without IFN-β (256, 1024 or 4096 IU/mL) for 48 or 72 h, fixed for 10 min in Carnoy's solution, and stained with hematoxylin-eosin (HE).

Quantitative analysis of IFN-β-induced apoptosis in vitro

Cells cultured with or without 1000 IU/mL (IFN-β) for 72 h were stained with Annexin V-enhanced green fluorescent protein (EGFP) apoptosis detection kits (Medical & Biological Laboratories, Nagoya, Japan) according to the manufacturer's protocol. After staining, the cells were analyzed using a FACScan (Becton Dickinson Immunocytometry Systems, San Jose, CA), and the Annexin V-EGFP-positive apoptotic cell rate was determined.

Effects of IFN-β on proliferation and expression of IFNAR-2 subunit

To investigate the expression of the IFNAR-2 subunit after contact with IFN-β, as well as its relationship with antiproliferative effects, HAK-1B cells were cultured with medium alone (control group) or medium containing 1000 IU/mL IFN-β for 3, 6, 12, 24, 48, or 72 h. The cells were reacted with anti-IFNAR-2 antibody (final concentration 2.5 μg/mL) or control antibody. The cell surface expression of the IFNAR-2 subunit was analyzed using flow cytometry with the technique described elsewhere,[20,21] with slight modification.

Effects of IFN-β on HCC cell proliferation in nude mice

This experiment was conducted according to the *Guide for the Care and Use of Laboratory Animals* published and revised by the National Institutes of Health in 1985. HAK-1B cells (1.0×10^7 cells/mouse) were transplanted subcutaneously (s.c.) into 4-week-old female BALB/c nu/nu athymic nude mice. Eight days later, when the largest diameter of the tumor reached approximately 5–10 mm, the mice were divided into four groups ($n = 10$ each) to balance the mean tumor diameter of each group. Each mouse received an intraperitoneal (i.p.) injection of 0.1 mL phosphate-buffered saline (PBS) containing 1,000, 10,000, or 100,000 IU IFN-β for 14 consecutive days. The clinical dose of IFN-β in chronic hepatitis C treatment is about 1.2×10^5 IU/kg and is 2.4 times the lowest dose (5.0×10^4 IU/kg) in the experiment. During this 2-week period, tumor size was measured in two directions using calipers once every 2 days until day 15, and tumor volume (mm^3) was estimated using the equation: length $\times$ (width)$^2 \times 0.5$. On day 15, the mice were killed, and the tumors were resected, weighed, and used for morphologic studies and ELISA analysis. Half of the resected tumor was fixed in formalin and prepared in paraffin sections. The TUNEL method using ApopTag kit (S7100, Chemicon) was used to detect apoptotic cells. The number of apoptotic cells was counted in ten 0.25-mm^2 areas where apoptotic cells

were present at relatively uniform density, and the average number per area was obtained. To compare the *in vivo* antitumor effect according to the administration route, IFN-β was administered i.v., and tumor volume and weight were examined as described.

Quantification of microvessel density

Double-immunostaining was performed with antimouse endothelial cell antibody, antihuman α-SMA antibody, Histofine simple stain mouse MAX-PO (Rat) kits (Nichirei, Tokyo, Japan), and HistoMouse-plus kits to detect arterylike blood vessels as described in our previous report.[21] The number of blood vessels in the tumor and in the borderline area between the tumor nodule and surrounding tissues was counted on each specimen. The size of the counted area was measured by tracing the outline displayed on a computer monitor using Mac SCOPE (Mitani Corp., Chiba, Japan). From the obtained number of vessels per unit area (mm^2), the group mean was obtained for group comparison.

Enzyme-linked immunosorbent assay (ELISA)

Portions of the resected tumors were cut into pieces, and an appropriate amount was homogenized in 500 μL ice-cold Ca^{2+}- and Mg^{2+}-free PBS containing 100 μg/mL phenymethylsulfonyl fluoride (PMSF) using a pellet pestle. The mixture was centrifuged for 10 min (12,000*g*, 4°C), and the supernatant was stored at −20°C until use. The amount of tissue protein was determined using BCA protein assay reagent (Pierce Biotechnology, Rockford, IL). The concentration in the samples was determined by comparing their absorbance with a standard curve. The amount of basic fibroblast growth factor (bFGF), interleukin-8 (IL-8), and vascular endothelial growth factor (VEGF) in the supernatant was measured using ELISA kits. The kits for VEGF and IL-8 were supplied by Amersham Biosciences (Buckinghamshire, U.K.), and those for bFGF by R&D Systems (Minneapolis, MN).

Effects of IFN-β and 5-FU on proliferation of HCC and CHC cell lines in vitro

The cells (1.5–6 × 10^3 cells/well) were seeded on 96-well plates and cultured for 24 h, and then the culture medium was changed to fresh medium containing IFN-β (0, 8, 40, 200, or 100 IU/mL), 5-FU (0, 1, 10, or 100 μM), or both IFN-β (0, 8, 40, 200, or 100 IU/mL) and 5-FU (0, 1, 10, or 100 μM). After 72 h of culture, the number of viable cells was examined with colorimetry using MTT assay kits as described. The synergy of cooperative cytotoxicity was determined by the median-effect principle as described by Chou and Talalay.[40] Data from each sample were analyzed using CalcuSyn ver. 2 (Biosoft, Cambridge, U.K.).

Statistical analysis

Estimated tumor volume and colorimetric cell growth were compared using two-factor factorial ANOVA and Student's *t*-test, respectively. The other data comparisons were performed using the Mann-Whitney U-test.

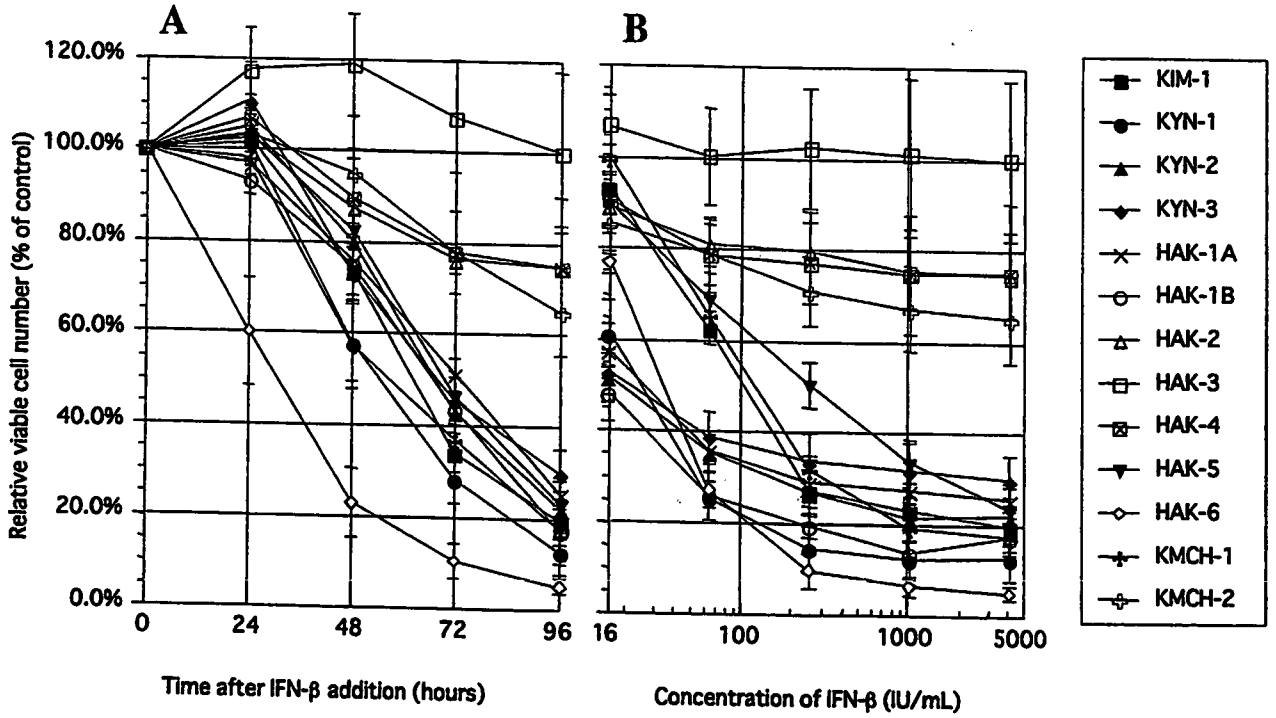

FIG. 1. Antiproliferative effect of IFN-β. (**A**) Chronologic changes in the relative viable cell number (% of the control) after adding 4096 IU/mL IFN-β. Growth was suppressed with time in 12 cell lines. (**B**) 96 h after adding 16, 64, 256, 1024, or 4,096 IU/mL IFN-β. Cell proliferation was suppressed in a dose-dependent manner in 11 cell lines. Suppression was statistically significant ($p < 0.001$–0.05) in the range of 16–4096 IU/mL IFN-β in 8 cell lines. Eight samples were used in each experiment ($n = 8$). The experiment was repeated at least three times for each cell line. The figures represent average ± SE of the experiments.

RESULTS

Effects of IFN-β on liver cancer cell proliferation in vitro

In 12 of the 13 cell lines, a time-dependent antiproliferative effect was observed at various degrees in the 96-h cultures with 4096 IU/mL of IFN-β, and 20% or more suppression occurred at 72 h or later in comparison to the control (Fig. 1A). Among the 12 cell lines, HAK-6 presented a different pattern, and the cell number started to decrease from the early culture period after the addition of IFN-β, decreasing to 60% of the control at 24 h. On the other hand, HAK-3 did not have suppressive effects at 96 h.

The relative viable cell number at 96 h after adding IFN-β (16, 64, 256, 1024, or 4096 IU/mL) decreased in 11 of the 13 cell lines in a dose-dependent manner (Fig. 1B). The cell lines that did not have effects were HAK-3 and HAK-4. Among the 11 cell lines, cell number was suppressed in the 6 cell lines (KYN-1, KYN-2, KYN-3, HAK-1A, HAK-1B, and HAK-6) to <40% of the control even at a very low dose (64 IU/mL), and the suppression was statistically significant in 8 cell lines in the dose range between 16 and 4096 IU/mL ($p < 0.001$–0.05). The 50% inhibitory concentration (IC_{50}) was 14.8 IU/mL for KYN-2, 15.4 for HAK-1B, 25.2 for KYN-3, 31.2 for KYN-1, 32.5 for HAK-1A, 42.0 for HAK-6, 132.0 for KIM-1, 152.7 for KMCH-1, and 260.1 for HAK-5. There was no significant relationship between the histologic differentiation level of the original tumor of each cell line and sensitivity to the antiproliferative effect of IFN-β.

Between 48 and 72 h after adding 4096 IU/mL IFN-β, 10 cell lines (all but HAK-3, HAK-4, and KMCH-2) presented such characteristic features of apoptosis as cytoplasmic shrinkage, chromatin condensation, and nuclear fragmentation to various degrees (Color Plate 1).

Quantitative analysis of Annexin V-EGFP-positive apoptotic cells revealed that apoptosis occurred at a significantly higher rate in the cultures with 1000 IU/mL IFN-β than those without IFN-β in 10 cell lines (Table 1).

Effects of IFN-β in vitro *on proliferation and expression of IFNAR-2 in HAK-1B cells*

With IFN-β, the expression of IFNAR-2 in HAK-1B cells was significantly downregulated in the period between 6 and 12 h in comparison to the control, then significantly upregulated at 48 h and returned to the control level at 72 h (Fig. 2). The number of viable cells between 3 and 12 h was almost the same in both the control and the culture with IFN-β, started to decrease after 24 h in the IFN-β group, and decreased to 16.1% of the control at 72 h.

Effects of IFN-β on HCC cell proliferation in nude mice

Figure 3A summarizes the chronologic changes in estimated tumor volume after s.c. injection of cultured HAK-1B cells to nude mice. A significant difference in the time course change was obtained between the control mice and the mice that received 1,000 ($p < 0.05$), 10,000 ($p < 0.0001$), or 100,000 IU ($p < 0.0001$) IFN-β by two-factor factorial ANOVA. Dose-dependent suppression of tumor volume was also observed, and HAK-1B tumor on day 15 was smaller in proportion to the dose (Fig. 3A). A significant difference was obtained in the tumor weight between the control and the 10,000 IU/mouse group ($p < 0.05$) and 100,000 IU/mouse group ($p < 0.001$). The tumor weight of the 100,000 IU/mouse group was 40.0% of the control. Similar antitumor effects were obtained when IFN-β was administered i.v. (data not shown).

TUNEL staining showed that the numbers of apoptotic cells in the 10,000 IU and 100,000 IU IFN-β groups were significantly higher than that of the control, and the number increased in a dose-dependent manner (Color Plate 2 and Table 2) ($p <$ 0.0001 between 10,000 or 100,000 group vs. Control).

Expression of angiogenesis factors and density of arterylike blood vessels

VEGF expression in the HAK-1B tumor was higher in mice that received IFN-β and was significantly higher in the 10,000 IU IFN-β group ($p < 0.05$) than the control (Table 2). IL-8 expression in the tumor was not significantly different among the groups. bFGF expressions in both tumor and serum were significantly lower in the 1,000 IFN-β group ($p < 0.05$) than the control, and IL-8 expressions in serum were significantly lower in all IFN-β groups ($p < 0.0001$).

There were no significant differences in the number of blood vessels per unit area of the HAK-1B tumor among all groups, but the blood vessel counts inside the tumor tended to be lower in the 1,000 IU IFN-β group (Table 2).

Antiproliferative effects of IFN treatment in combination with 5-FU

Seventy-two hours after the addition of 5-FU alone, the relative viable cell number was suppressed in all 13 cell lines in a dose-dependent manner. The combination treatment of IFN-β and 5-FU showed synergistic antiproliferative effects in all

TABLE 1. QUANTITATIVE ANALYSIS OF APOPTOSIS INDUCED BY IFN-β IN 13 LIVER CANCER CELL LINES[a]

Cell line	*Annexin V-EGFP-positive apoptotic cells (%)*	
	Control	*IFN-β*
KIM-1	6.9 ± 3.6	36.2 ± 2.3**
KYN-1	10.2 ± 0.7	24.2 ± 1.3**
KYN-2	8.1 ± 1.3	28.2 ± 4.3**
KYN-3	6.3 ± 1.5	17.1 ± 3.7**
HAK-1A	8.7 ± 0.8	19.1 ± 0.7**
HAK-1B	8.7 ± 3.7	30.4 ± 2.9**
HAK-2	11.9 ± 2.4	21.6 ± 1.9*
HAK-3	4.8 ± 0.9	8.9 ± 1.5
HAK-4	5.9 ± 2.3	6.9 ± 0.8
HAK-5	3.7 ± 0.5	20.9 ± 1.9**
HAK-6	11.5 ± 2.9	33.6 ± 2.6**
KMCH-1	6.5 ± 1.0	18.3 ± 1.2**
KMCH-2	7.8 ± 2.6	7.4 ± 3.0

[a]Cells were cultured with medium alone (Control) or medium with 1000 IU/mL IFN-β. Apoptosis was measured by Annexin V-EGFP staining. The rates of Annexin V-EGFP-positive apoptotic cells are shown as the average ± SD. Five samples were used in each experiment.

*$p < 0.001$ vs. corresponding control value.

**$p < 0.0001$ vs. corresponding control value.

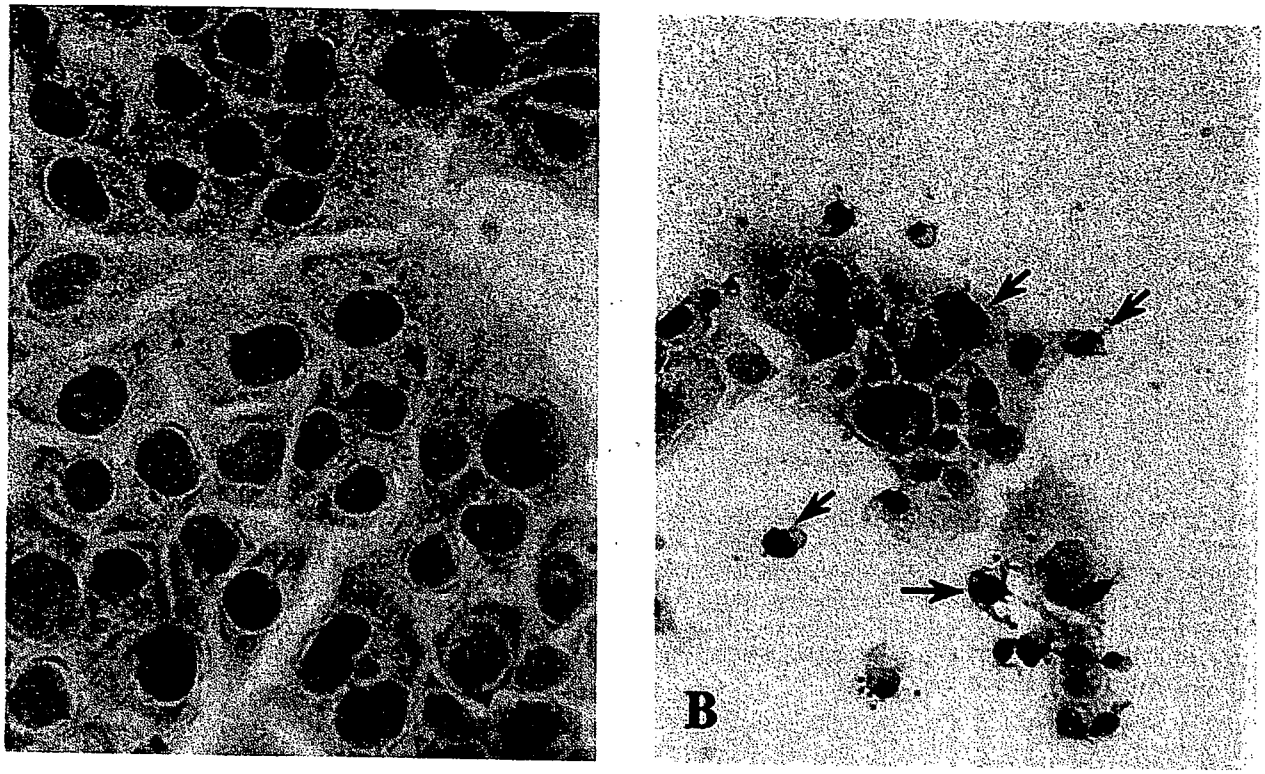

COLOR PLATE 1. Photomicrograph of HAK-1B cells cultured for 48 h on a Lab-Tek chamber slide (**A**) without IFN-β in culture medium and (**B**) with 4096 IU/mL IFN-β in culture medium. Apoptotic cells (arrows) characterized by cytoplasmic shrinkage, chromatic condensation, and nuclear fragmentation were noted. HE staining ×200.

cell lines, but the frequency of the effect and the suitable combination of each drug concentration depended on the cell lines. Synergistic effects were observed most frequently at 10 μM 5-FU in all cell lines excluding KMCH-2 (Fig. 4); however, in three cell lines (HAK-1A, HAK-1B, and HAK-2), synergistic effects were observed with high frequency at all 5-FU concentrations tested.

DISCUSSION

This study showed that (1) a time-dependent antiproliferative effect was induced in 12 cell lines that had contact with 4096 IU/mL IFN-β for 24–96 h and (2) a dose-dependent antiproliferative effect was induced in 11 cell lines *in vitro* in the range of 16–4096 IU/mL. We previously reported the antipro-

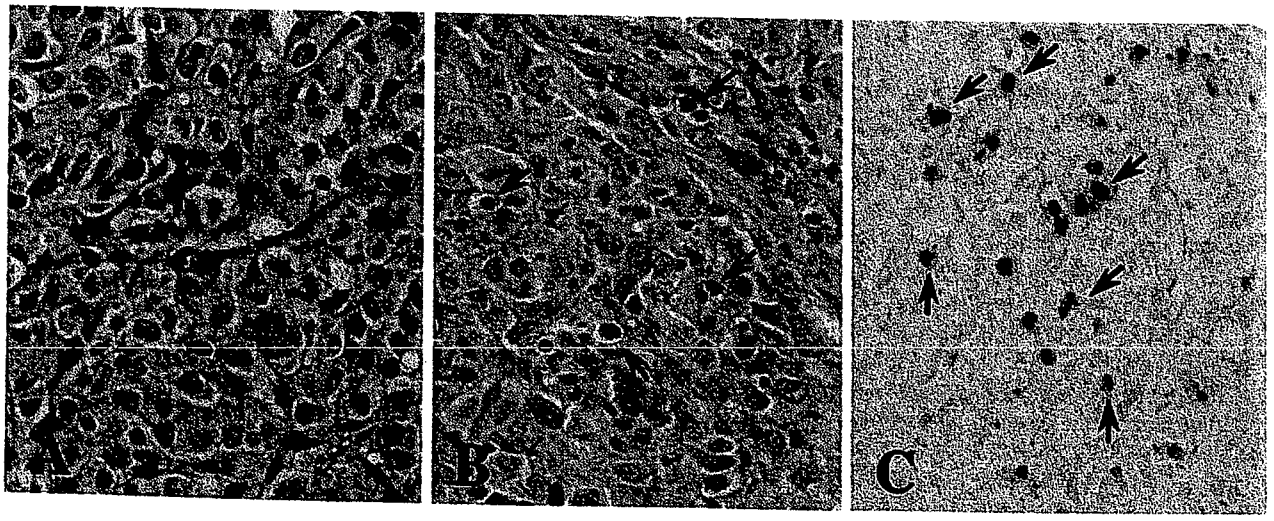

COLOR PLATE 2. Photomicrograph of subcutaneous human HCC tumor in nude mice that developed after the injection of HAK-1B cells. (**A**) Control mouse that received culture medium alone. Tumor shows a thick trabecular arrangement of tumor cells and a sinusoidlike structure in the stroma. (**B**) Mouse that received an i.p. injection of 100,000 IU IFN-β. There are many apoptotic tumor cells (arrows). HE staining. ×200. (**C**) TUNEL technique was used to identify apoptotic cells (arrows). Counterstained with Mayer's hematoxylin. ×200.

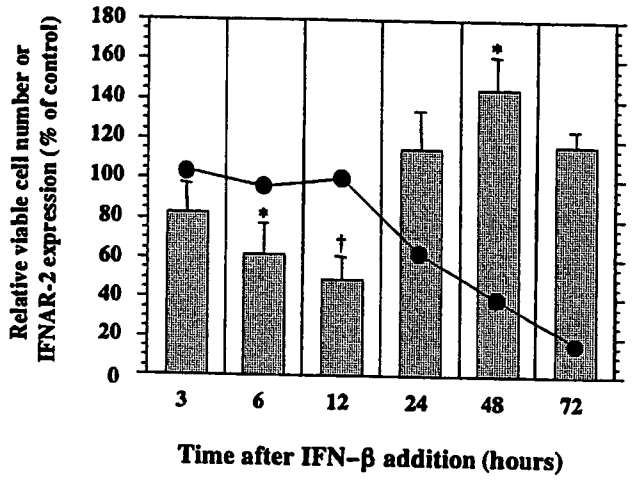

FIG. 2. Effects of 1000 IU/mL IFN-β. Time course changes in the relative viable cell number (circles, % of control) and IFNAR-2 expression in HAK-1B cells before and after the addition of 1000 IU/mL IFN-β ($n = 5$ at each measurement). The figures represent the average ± SE. *$p < 0.05$ vs. corresponding control value; †$p < 0.005$ vs. corresponding control value. The experiment was repeated three times.

liferative effects of three IFN-α preparations by using the same cell lines and methods.[20,21,24] Comparison between previous findings on IFN-α preparations and the current findings on IFN-β showed that (1) IFN-β induced a time-dependent antiproliferative effect in the largest number of cell lines, (2) in the 96-h culture with 1024 IU/mL IFN-β, the relative viable cell number became lower than 50% in 9 cell lines, and this was also the largest number of cell lines in our IFN studies, and (3) in 6 of the 9 cell lines, growth suppression occurred at a dose <100 IU/mL, and the IC_{50} of the 9 cell lines ranged between 14.8 and 260.1 IU/mL, lower than the levels for the 3 IFN-α preparations.[20,21,24] For example, in HAK-1B cells, the IC_{50s} of the 3 IFN-α preparations (i.e., BALL-1 lymphoblastoid IFN-α, consensus IFN-α, and PEG-IFN-α2b)[20,21,24] were 14, 43, and 55 times higher, respectively, than the IC50 of IFN-β. In various cell lines, such as melanoma and glioma, IFN-β presents a stronger antiproliferative effect than IFN-α even though IFN-α and IFN-β bind to the same heterodimeric receptor.[41–43] Leaman et al.[44] conducted oligonucleotide array analysis on 2 melanoma cell lines and showed that IFN-β was more potent than IFN-α2 in the induction of IFN-stimulated gene (ISG) expression. In HCC cell lines, there have been different findings, that is, IFN-β induced a stronger antiproliferative effect and higher ISG expression than IFN-α,[29,30] and neither IFN-α nor IFN-β significantly inhibited the growth of liver cancer cells.[28] We presume that this difference is attributable to differences in the IFN preparations and experiment methods, and particularly to differences in the cell lines used in the experiments. The 4 cell lines (HAK-2, HAK-3, HAK-4, KMCH-2) whose relative viable cell numbers in the current study were higher than 50% after 96-h exposure to 4096 IU/mL IFN-β were found to be also relatively insensitive to the antiproliferative effect of 3 IFN-α preparations.[20,21,24] IFN-β-mediated apoptosis induction was observed as an antiproliferative mechanism in 10 cell lines but not in the other 3 cell lines (HAK-3, HAK-4, KMCH-2). The low sensitivity or insensitivity to the antiproliferative effect of IFN-β in the 4 cell lines (HAK-2, HAK-3, HAK-4, KMCH-2) would be attributable to the resistance to IFN-β-mediated apoptosis or low cell surface IFNAR-2 expression (HAK-3, HAK-4, KMCH-2).[20]

IFN-β induces a stronger antiproliferative effect and higher ISG expression than IFN-α. It has been reported that the different biologic effects of IFN-β from those of IFN-α2 may be mediated by the formation of a uniquely stable type I IFN receptor complex, greater affinity for the type I receptor complex, involvement of other receptor components, and the activation of additional signaling pathways.[45–47] These findings suggest

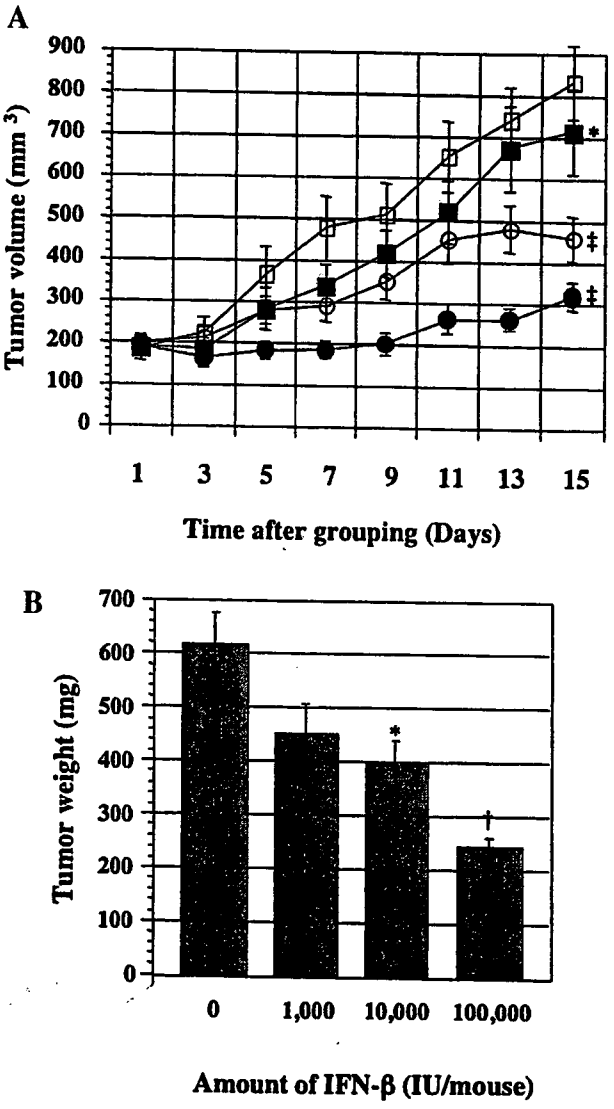

FIG. 3. Time course change in estimated tumor volume of s.c. transplanted HAK-1B in nude mice. (A) Mice received an s.c. injection of 1,000 (closed squares), 10,000 (open circles), or 100,000 (closed circles) IU IFN-β or PBS (control, open squares). (B) All mice were killed on day 15, and tumor weight was measured. Figures represent the average ± SE. The experiments were repeated twice, and almost identical results were obtained. *$p < 0.05$ vs. control; †$p < 0.001$ vs. control; ‡$p < 0.0001$ vs. control.

TABLE 2. ELISA, ARTERYLIKE BLOOD VESSELS, AND NUMBER OF APOPTOTIC CELLS IN HUMAN HCC (HAK-1B) TUMOR THAT WAS SUBCUTANEOUSLY TRANSPLANTED IN NUDE MICE

Treatment group[a]	*Control*	*IFN-β 1,000 IU*	*IFN-β 10,000 IU*	*IFN-β 100,000 IU*
VEGF[b] in tumor	20.0 ± 3.0[c]	27.7 ± 4.8	30.1 ± 3.2*	22.6 ± 3.9
bFGF[b] in tumor	46.8 ± 2.9	38.4 ± 4.6*	39.1 ± 1.7	48.6 ± 2.6
in serum	16.0 ± 4.4	6.2 ± 1.4*	7.8 ± 1.6	3.6 ± 0.4*
IL-8[b] in tumor	35.8 ± 3.2	37.3 ± 3.0	39.6 ± 3.5	36.7 ± 2.5
in serum	27.0 ± 2.2	11.0 ± 2.4**	10.9 ± 1.7***	8.1 ± 1.4***
Arterylike blood vessel[d]				
inside tumor	0.381 ± 0.074	0.318 ± 0.053	0.390 ± 0.075	0.413 ± 0.057
tumor margin	0.621 ± 0.081	0.646 ± 0.069	0.770 ± 0.128	0.701 ± 0.077
Apoptotic cell[e]	67.2 ± 5.2	73.9 ± 3.8	113.4 ± 5.4***	155.1 ± 7.9***

[a]Cultured HAK-1B cells (1×10^7) were transplanted s.c. into nude mice. Eight days later, when the largest diameter of the tumor reached approximately 5–10 mm, mice in each group were treated every day with i.p. injections of IFN-β or saline (Control).

[b]ELISA data (VEGF, bFGF, and IL-8) are expressed as ng/100 pg total protein.

[c]Average ± SE.

[d]Arterylike blood vessels: number of blood vessels in the tumor and in the borderline area between the tumor nodule and surrounding tissues was counted in each specimen, and the average number per area in each group was obtained.

[e]Number of apoptotic cells was counted in eight 0.25-mm^2 areas in each section, and the average number per area in each group was obtained.

*$p < 0.05$ vs. Control; **$p < 0.005$ vs. Control; ***$p < 0.001$ vs. Control.

that the difference in such effects as antiproliferation and potency between IFN-α and IFN-β may be largely related to the different interaction with type I IFN receptor. We recently examined chronologic changes in IFNAR-2 expression in HAK-1B cells cultured with PEG-IFN-α2b and found that the expression of IFNAR-2 was significantly downregulated at 3 h compared with the control, then significantly upregulated at 48 h, and returned to the control level at 72 h.[21] In the current study, we also examined chronologic changes of IFNAR-2 expression with IFN-β by using the same HCC cell line, HAK-1B, for up to 72 h of culture and compared the current results with the previous results on PEG-IFN-α2b. As a result, IFNAR-2 expression after IFN-α or IFN-β exposure was not different, and we could not find a difference at this point.

IFN-β *in vivo* dose-dependently suppressed the growth of human HCC that was transplanted s.c. to nude mice, and growth suppression occurred even at 1/2.4 of the clinical dose for chronic hepatitis C patients. By considering the IC_{50} of *in vitro* IFN-β that was 1/43 of the consensus IFN-α[24] and by comparing to our previous *in vivo* findings of consensus IFN-α,[24] IFN-β is expected to have much stronger antiproliferative effects than those found in the current results. There was no difference in the antiproliferative effects between the i.p. and i.v. administrations of IFN-β. The reason for this lower level of antiproliferative effects has not yet been described fully, but pharmacokinetic studies indicate that IFN-β exhibits an extremely short half-life in the blood system after i.m. or i.v. protein administration.[48,49] Therefore, the short half-life of IFN-β in serum may be related to the *in vivo* findings.

In our recent study on PEG-IFN-α2b and IFN-α2b, which are equal in their antivirus activity level,[21] their *in vivo* antiproliferative effects on HCC were comparatively examined. The antiproliferative effect was significantly higher in PEG-IFN-α2b, with a longer serum half-life than IFN-α2b. This suggested that the antitumor effect is higher when IFN is present in the serum for a longer time. Similar findings were reported for IFN-β. In clinical practice, the clearance rate of serum HCV RNA and the ratio of 2′,5′-oligoadenylate synthetase (2′,5′-OAS) activity were significantly higher in chronic hepatitis patients who received 3 MU IFN-β i.v. twice a day than those who received 6 MU IFN-β daily.[50,51] In animal experiments, Sung et al.[52] examined the pharmacokinetic properties of albuferon in rhesus monkeys. Albuferon is a novel recombinant protein derived from the gene fusion of IFN-β and human serum albumin, and its half-life is longer than that of IFN-β. They found an enhanced pharmacodynamic response, with increases in both neopterin and 2′,5′-OAS expression levels. Therefore, it is necessary to conduct further *in vivo* studies that use a more frequent administration of IFN-β or IFN-β with a longer half-life.

Our current study examined the mechanism of *in vivo* antiproliferative effects by monitoring apoptosis, angiogenesis, and the expression of angiogenesis factors. As a result, the number of apoptotic cells increased with the increase in the IFN-β dose, and this showed the occurrence of antiproliferation due to apoptosis induction, as was found for IFN-α.[22,24] On the other hand, angiogenesis inhibition was not observed as well as for PEG-IFN-α2b[21]; that is, the number of blood vessels in and around the tumor did not decrease significantly. Several studies reported that IFN-β inhibits angiogenesis by suppressing the expression of such angiogenesis factors as bFGF[53,54] and IL-8.[55,56] However, in the current study, decreased expression of bFGF and IL-8 in the serum of IFN-β groups, in particular the 100,000 IU group, was thought to be the result of tumor size reduction. Regarding the expressions in nude mouse tumors, IL-8 expression was not significantly different among the groups, and VEGF expression was significantly increased in the 10,000 IU IFN-β group. In the 1,000 IU group,

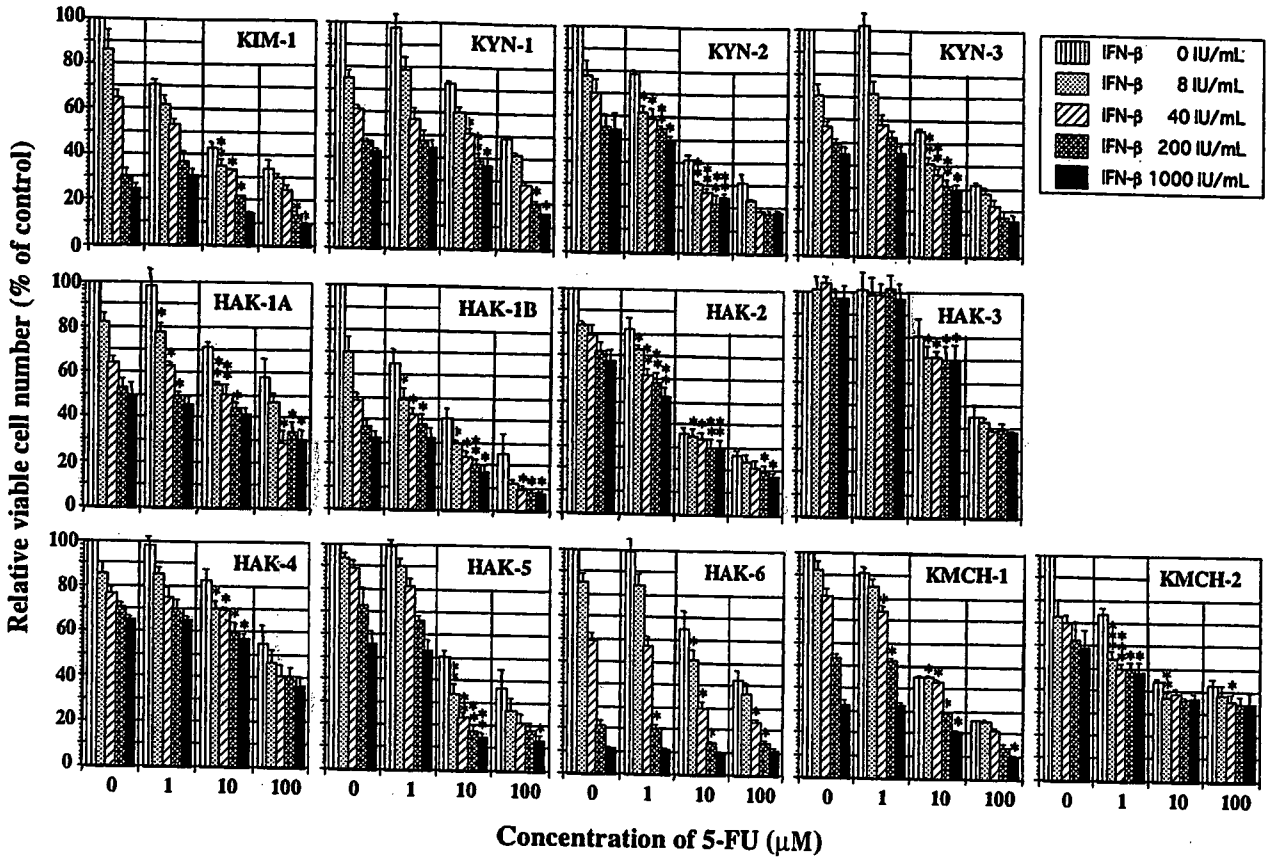

FIG. 4. Antiproliferative effect of IFN-β in combination with various doses of 5-FU. Cells were incubated with IFN-β in the presence of various concentrations of 5-FU, and a relative viable cell number (% of control) was determined after 72 h of culture. Eight samples were used in each experiment, which was repeated at least three times for each cell line. Figures represent the average ± SE. *Synergistic effect with the range of the combination index (CI) of 0.3–0.7; **strong synergistic effect with the range of the CI of 0.1–0.3; ***very strong synergistic effect with the range of CI of <0.1. Synergistic effects and the CI were assessed by median-effect principle analysis.

bFGF expression decreased significantly from the level of the control, and the number of blood vessels decreased inside the tumor. Therefore, bFGF and blood vessels might be related, and in the 1,000 IU group, IFN could suppress the expression of angiogenesis factors at a biologically optimal concentration as Tedjarati et al.[57] reported, even though there was no specific decrease in tumor size. VEGF expression in HAK-1B cells *in vitro* was upregulated in the same manner as for IFN-α.[58]

The clinical efficacy of chemotherapy in combination with IFN-α has already been reported in HCC.[17–19] As *in vitro* data suggest that the antiproliferative potency of IFN-β is greater than that of IFN-α,[41–43] IFN-β in combination with chemotherapeutic drugs would be a more promising therapeutic approach in the treatment of HCC. Makower and Wadler[59] described that IFN-β is a more potent modulator of 5-FU cytotoxicity *in vitro* than IFN-α. In the current study, we examined the cooperative effects of IFN-β with 5-FU on 13 human liver cancer cell lines using growth inhibitory assays and median-effect principle analyses and found synergistic antiproliferative effects in all cell lines at various degrees. The possible reported mechanisms of these synergistic effects are as follows[59–61]: (1) IFN-β may increase the amount of active 5-FU metabolite and inhibit the activity of thymidylate synthase, (2) IFN-β may alter the expression of enzymes that affect 5-FU metabolism (e.g., thymidine phosphorylase, dihydropyrimidine dehydrogenase, uridine phosphorylase, and thymidine kinase), and (3) 5-FU may upregulate the expression levels of type I IFN receptor subunits. Oie et al.[61] examined the mechanisms of the antiproliferative effect of combination treatment with IFN-α and 5-FU by using 6 HCC cell lines and confirmed that the upregulation of type I IFN receptor by 5-FU is the most important mechanism of synergistic effects.

Our findings showed that IFN-β even at a relatively low dose has a potent antiproliferative effect on HCC *in vitro*, and the *in vivo* antitumor effect was expressed at the clinical dose. These data suggest the potential clinical application of IFN-β in the prevention and treatment of HCC. Strong growth suppression on HCC could be expected when a relatively low dose of IFN-β with or without 5-FU is continuously or frequently administered to tumor-feeding arteries of HCC.

ACKNOWLEDGMENTS

We thank Ms. Akemi Fujiyoshi for her assistance in our experiments and Dr. Tomohiko Suzuki (Toray Industries, Ltd.) for his assistance in data analysis. This study was supported in part by the Sarah Cousins Memorial Fund, Boston, Massachu-

setts, and by a grant-in-aid from the Ministry of Health, Labor and Welfare of Japan (17200501).

REFERENCES

1. Stark JJ, Dillman RO, Schulof R, Wiemann MC, Barth NM, Honeycutt PJ, Soori G. Interferon-α and chemohormonal therapy for patients with advanced melanoma: final results of a phase I–II study of the Cancer Biotherapy Research Group and the Mid-Atlantic Oncology Program. *Cancer* 1998;82:1677–1681.
2. Xu D, Erickson S, Szeps M, Gruber A, Sangfelt O, Einhorn S, Pisa P, Grander D. Interferon α down-regulates telomerase reverse transcriptase and telomerase activity in human malignant and nonmalignant hematopoietic cells. *Blood* 2000;96:4313–4318.
3. Pestka S, Langer JA, Zoon KC, Samuel CE. Interferons and their actions. *Annu. Rev. Biochem.* 1987;56:727–777.
4. Sen GC, Lengyel P. The interferon system—a bird's eye view of its biochemistry. *J. Biol. Chem.* 1992;267:5017–5020.
5. Rani MR, Ransohoff RM. Alternative and accessory pathways in the regulation of IFN-β-mediated gene expression. *J. Interferon Cytokine Res.* 2005;25:788–798.
6. Brechot C, Jaffredo F, Lagorce D, Gerken G, Meyer zum Buschenfelde K, Papakonstontinou A, Hadziyannis S, Romeo R, Colombo M, Rodes J, Bruix J, Williams R, Naoumov N. Impact of HBV, HCV and GBV-C/HGV on hepatocellular carcinomas in Europe: results of a European concerted action. *J. Hepatol.* 1998;29:173–183.
7. Di Bisceglie AM, Order SE, Klein JL, Waggoner JG, Sjogren MH, Kuo G, Houghton M, Choo QL, Hoofnagle JH. The role of chronic viral hepatitis in hepatocellular carcinoma in the United States. *Am. J. Gastroenterol.* 1991;86:335–338.
8. Shiratori Y, Shiina S, Imamura M, Kato N, Kanai F, Okudaira T, Teratani T, Tohgo G, Toda N, Ohashi M, Ogura K, Niwa Y, Kawabe T, Omata M. Characteristic difference of hepatocellular carcinoma between hepatitis B- and C-viral infection in Japan. *Hepatology* 1995;22:1027–1033.
9. Ikeda K, Saitoh S, Arase Y, Chayama K, Suzuki Y, Kobayashi M, Tsubota A, Nakamura I, Murashima N, Kumada H, Kawanishi M. Effect of interferon therapy on hepatocellular carcinogenesis in patients with chronic hepatitis type C: a long-term observation study of 1,643 patients using statistical bias correction with proportional hazard analysis. *Hepatology* 1999;29:1124–1130.
10. Ikeda K, Arase Y, Saitoh S, Kobayashi M, Suzuki Y, Suzuki F, Tsubota A, Chayama K, Murashima N, Kumada H. Interferon beta prevents recurrence of hepatocellular carcinoma after complete resection or ablation of the primary tumor—a prospective randomized study of hepatitis C virus-related liver cancer. *Hepatology* 2000;32:228–232.
11. Mazzella G, Accogli E, Sottili S, Festi D, Orsini M, Salzetta A, Novelli V, Cipolla A, Fabbri C, Pezzoli A, Roda E. Alpha interferon treatment may prevent hepatocellular carcinoma in HCV-related liver cirrhosis. *J. Hepatol.* 1996;24:141–147.
12. Nishiguchi S, Kuroki T, Nakatani S, Morimoto H, Takeda T, Nakajima S, Shiomi S, Seki S, Kobayashi K, Otani S. Randomised trial of effects of interferon-α on incidence of hepatocellular carcinoma in chronic active hepatitis C with cirrhosis. *Lancet* 1995;346:1051–1055.
13. Sakaguchi Y, Kudo M, Fukunaga T, Minami Y, Chung H, Kawasaki T. Low-dose, long-term, intermittent interferon-alpha-2b therapy after radical treatment by radiofrequency ablation delays clinical recurrence in patients with hepatitis C virus-related hepatocellular carcinoma. *Intervirology* 2005;48:64–70.
14. Johnson PJ. Hepatocellular carcinoma: is current therapy really altering outcome? *Gut* 2002;51:459–462.
15. Gutterman JU. Cytokine therapeutics: lessons from interferon α. *Proc. Natl. Acad. Sci. USA* 1994;91:1198–1205.
16. Negrier S, Escudier B, Lasset C, Douillard JY, Savary J, Chevreau C, Ravaud A, Mercatello A, Peny J, Mousseau M, Philip T, Tursz T. Recombinant human interleukin-2, recombinant human interferon alfa-2a, or both in metastatic renal-cell carcinoma. Groupe Francais d'Immunotherapie. *N. Engl. J. Med.* 1998;338:1272–1278.
17. Leung TW, Tang AM, Zee B, Yu SC, Lai PB, Lau WY, Johnson PJ. Factors predicting response and survival in 149 patients with unresectable hepatocellular carcinoma treated by combination cisplatin, interferon-alpha, doxorubicin and 5-fluorouracil chemotherapy. *Cancer* 2002;94:421–427.
18. Sakon M, Nagano H, Dono K, Nakamori S, Umeshita K, Yamada A, Kawata S, Imai Y, Iijima S, Monden M. Combined intraarterial 5-fluorouracil and subcutaneous interferon-α therapy for advanced hepatocellular carcinoma with tumor thrombi in the major portal branches. *Cancer* 2002;94:435–442.
19. Urabe T, Kaneko S, Matsushita E, Unoura M, Kobayashi K. Clinical pilot study of intrahepatic arterial chemotherapy with methotrexate, 5-fluorouracil, cisplatin and subcutaneous interferon-alpha-2b for patients with locally advanced hepatocellular carcinoma. *Oncology* 1998;55:39–47.
20. Yano H, Iemura A, Haramaki M, Ogasawara S, Takayama A, Akiba J, Kojiro M. Interferon alfa receptor expression and growth inhibition by interferon alfa in human liver cancer cell lines. *Hepatology* 1999;29:1708–1717.
21. Yano H, Ogasawara S, Momosaki S, Akiba J, Kojiro S, Fukahori S, Ishizaki H, Kuratomi K, Basaki Y, Oie S, Kuwano M, Kojiro M. Growth inhibitory effects of pegylated IFN α-2b on human liver cancer cells *in vitro* and *in vivo*. *Liver Int.* 2006;26:964–975.
22. Yano H, Yanai Y, Momosaki S, Ogasawara S, Akiba J, Kojiro S, Moriya F, Fukahori S, Kuruimoto M, Kojiro M. Growth inhibitory effects of interferon-α subtypes vary according to human liver cancer cell lines. *J. Gastroenterol. Hepatol.* 2006;21:1720–1725.
23. Yano H, Ogasawara S, Momosaki S, Akiba J, Nishida N, Kojiro S, Ishizaki H, Kojiro M. Expression and activation of apoptosis-related molecules involved in interferon-α-mediated apoptosis in human liver cancer cells. *Int. J. Oncol.* 2005;26:1645–1652.
24. Hisaka T, Yano H, Ogasawara S, Momosaki S, Nishida N, Takemoto Y, Kojiro S, Katafuchi Y, Kojiro M. Interferon-αCon1 suppresses proliferation of liver cancer cell lines *in vitro* and *in vivo*. *J. Hepatol.* 2004;41:782–789.
25. Huber BE, Wirth PJ, Newbold JE. Effects of human lymphoblastoid interferon on proliferation, gene expression and tumourigenicity of human hepatoma cell lines. *Drugs Exp. Clin. Res.* 1991;17:281–291.
26. Dunk AA, Ikeda T, Pignatelli M, Thomas HC. Human lymphoblastoid interferon. *In vitro* and *in vivo* studies in hepatocellular carcinoma. *J. Hepatol.* 1986;2:419–429.
27. Murphy D, Detjen KM, Welzel M, Wiedenmann B, Rosewicz S. Interferon-α delays S-phase progression in human hepatocellular carcinoma cells via inhibition of specific cyclin-dependent kinases. *Hepatology* 2001;33:346–356.
28. Matsumoto K, Okano J, Murawaki Y. Differential effects of interferon alpha-2b and beta on the signaling pathways in human liver cancer cells. *J. Gastroenterol.* 2005;40:722–732.
29. Damdinsuren B, Nagano H, Sakon M, Kondo M, Yamamoto T, Umeshita K, Dono K, Nakamori S, Monden M. Interferon-β is more potent than interferon-α in inhibition of human hepatocellular carcinoma cell growth when used alone and in combination with anticancer drugs. *Ann. Surg. Oncol.* 2003;10:1184–1190.
30. Murata M, Nabeshima S, Kikuchi K, Yamaji K, Furusyo N, Hayashi J. A comparison of the antitumor effects of interferon-α and β on human hepatocellular carcinoma cell lines. *Cytokine* 2006;33:121–128.
31. Yano H, Kojiro M, Nakashima T. A new human hepatocellular carcinoma cell line (KYN-1) with a transformation to adenocarcinoma. *In Vitro Cell. Dev. Biol.* 1986;22:637–646.
32. Yano H, Maruiwa M, Murakami T, Fukuda K, Ito Y, Sugihara S, Kojiro M. A new human pleomorphic hepatocellular carcinoma cell line, KYN-2. *Acta Pathol. Jpn.* 1988;38:953–966.

33. Murakami T. Establishment and characterizatin of human hepatoma cell line (KIM-1). *Acta Hepatol. Jpn.* 1984;25:532–539.
34. Murakami T, Maruiwa M, Fukuda K, Kojiro M, Tanaka M, Tanikawa K. Characterization of a new human hepatoma cell line (KYN-3) derived from the ascites of the hepatoma patient [Abstract]. *Jpn. J. Cancer Res.* 1988; Proceedings of the Japanese Cancer Association: 292.
35. Murakami T, Yano H, Maruiwa M, Sugihara S, Kojiro M. Establishment and characterization of a human combined hepatocholangiocarcinoma cell line and its heterologous transplantation in nude mice. *Hepatology* 1987;7:551–556.
36. Yano H, Iemura A, Fukuda K, Mizoguchi A, Haramaki M, Kojiro M. Establishment of two distinct human hepatocellular carcinoma cell lines from a single nodule showing clonal dedifferentiation of cancer cells. *Hepatology* 1993;18:320–327.
37. Yano H, Iemura A, Haramaki M, Momosaki S, Ogasawara S, Higaki K, Kojiro M. A human combined hepatocellular and cholangiocarcinoma cell line (KMCH-2) that shows the features of hepatocellular carcinoma or cholangiocarcinoma under different growth conditions. *J. Hepatol.* 1996;24:413–422.
38. Utsunomiya I, Iemura A, Yano H, Akiba J, Kojiro M. Establishment and characterization of a new human hepatocellular carcinoma cell line, HAK-3, and its response to growth factors. *Int. J. Oncol.* 1999;15:669–675.
39. Haramaki M, Yano H, Iemura A, Momosaki S, Ogasawara S, Inoue M, Yamaguchi R, Kusaba A, Utsunomiya I, Kojiro M. A new human hepatocellular carcinoma cell line (HAK-2) forms various structures in collagen gel matrices. *Hum. Cell* 1997;10:183–192.
40. Chou T-C, Talalay P. Analysis of combined drug effects: a new look at a very old problem. *Trends Pharmacol. Sci.* 1983;4:450–454.
41. Borden EC, Hogan TF, Voelkel JG. Comparative antiproliferative activity *in vitro* of natural interferons α and β for diploid and transformed human cells. *Cancer Res.* 1982;42:4948–4953.
42. Bradley NJ, Darling JL, Oktar N, Bloom HJ, Thomas DG, Davies AJ. The failure of human leukocyte interferon to influence the growth of human glioma cell populations: *in vitro* and *in vivo* studies. *Br. J. Cancer* 1983;48:819–825.
43. Chawla-Sarkar M, Leaman DW, Borden EC. Preferential induction of apoptosis by interferon (IFN)-β compared with IFN-α2: correlation with TRAIL/Apo2L induction in melanoma cell lines. *Clin. Cancer Res.* 2001;7:1821–1831.
44. Leaman DW, Chawla-Sarkar M, Jacobs B, Vyas K, Sun Y, Ozdemir A, Yi T, Williams BR, Borden EC. Novel growth and death related interferon-stimulated genes (ISGs) in melanoma: greater potency of IFN-β compared with IFN-α2. *J. Interferon Cytokine Res.* 2003;23:745–756.
45. Domanski P, Nadeau OW, Platanias LC, Fish E, Kellum M, Pitha P, Colamonici OR. Differential use of the βL subunit of the type I interferon (IFN) receptor determines signaling specificity for IFNα2 and IFNβ. *J. Biol. Chem.* 1998;273:3144–3147.
46. Ruzicka FJ, Jach ME, Borden EC. Binding of recombinant-produced interferon β ser to human lymphoblastoid cells. Evidence for two binding domains. *J. Biol. Chem.* 1987;262:16142–16149.
47. Russell-Harde D, Wagner TC, Perez HD, Croze E. Formation of a uniquely stable type I interferon receptor complex by interferon β is dependent upon particular interactions between interferon β and its receptor and independent of tyrosine phosphorylation. *Biochem. Biophys. Res. Commun.* 1999;255:539–544.
48. Salmon P, Le Cotonnec JY, Galazka A, Abdul-Ahad A, Darragh A. Pharmacokinetics and pharmacodynamics of recombinant human interferon-β in healthy male volunteers. *J. Interferon Cytokine Res.* 1996;16:759–764.
49. Fierlbeck G, Ulmer A, Schreiner T, Stroebel W, Schiebel U, Brzoska J. Pharmacodynamics of recombinant IFN-β during long-term treatment of malignant melanoma. *J. Interferon Cytokine Res.* 1996;16:777–781.
50. Shiratori Y, Perelson AS, Weinberger L, Imazeki F, Yokosuka O, Nakata R, Ihori M, Hirota K, Ono N, Kuroda H, Motojima T, Nishigaki M, Omata M. Different turnover rate of hepatitis C virus clearance by different treatment regimen using interferon-beta. *J. Hepatol.* 2000;33:313–322.
51. Ikeda F, Shimomura H, Miyake M, Fujioka SI, Itoh M, Takahashi A, Iwasaki Y, Sakaguchi K, Yamamoto K, Higashi T, Tsuji T. Early clearance of circulating hepatitis C virus enhanced by induction therapy with twice-a-day intravenous injection of IFN-β. *J. Interferon Cytokine Res.* 2000;20:831–836.
52. Sung C, Nardelli B, LaFleur DW, Blatter E, Corcoran M, Olsen HS, Birse CE, Pickeral OK, Zhang J, Shah D, Moody G, Gentz S, Beebe L, Moore PA. An IFN-β-albumin fusion protein that displays improved pharmacokinetic and pharmacodynamic properties in nonhuman primates. *J. Interferon Cytokine Res.* 2003;23:25–36.
53. Izawa JI, Sweeney P, Perrotte P, Kedar D, Dong Z, Slaton JW, Karashima T, Inoue K, Benedict WF, Dinney CP. Inhibition of tumorigenicity and metastasis of human bladder cancer growing in athymic mice by interferon-β gene therapy results partially from various antiangiogenic effects including endothelial cell apoptosis. *Clin. Cancer Res.* 2002;8:1258–1270.
54. Singh RK, Llansa N, Bucana CD, Sanchez R, Koura A, Fidler IJ. Cell density-dependent regulation of basic fibroblast growth factor expression in human renal cell carcinoma cells. *Cell Growth Differ.* 1996;7:397–404.
55. Oliveira IC, Sciavolino PJ, Lee TH, Vilcek J. Downregulation of interleukin 8 gene expression in human fibroblasts: unique mechanism of transcriptional inhibition by interferon. *Proc. Natl. Acad. Sci. USA* 1992;89:9049–9053.
56. Singh RK, Gutman M, Llansa N, Fidler IJ. Interferon-β prevents the upregulation of interleukin-8 expression in human melanoma cells. *J. Interferon Cytokine Res.* 1996;16:577–584.
57. Tedjarati S, Baker CH, Apte S, Huang S, Wolf JK, Killion JJ, Fidler IJ. Synergistic therapy of human ovarian carcinoma implanted orthotopically in nude mice by optimal biological dose of pegylated interferon α combined with paclitaxel. *Clin. Cancer Res.* 2002;8:2413–2422.
58. Yamaguchi R, Yano H, Iemura A, Ogasawara S, Haramaki M, Kojiro M. Expression of vascular endothelial growth factor in human hepatocellular carcinoma. *Hepatology* 1998;28:68–77.
59. Makower D, Wadler S. Interferons as biomodulators of fluoropyrimidines in the treatment of colorectal cancer. *Semin. Oncol.* 1999;26:663–671.
60. Kreuser ED, Wadler S, Thiel E. Biochemical modulation of cytotoxic drugs by cytokines: molecular mechanisms in experimental oncology. *Recent Results Cancer Res.* 1995;139:371–382.
61. Oie S, Ono M, Yano H, Maruyama Y, Terada T, Yamada Y, Ueno T, Kojiro M, Hirano K, Kuwano M. The upregulation of type I interferon receptor gene plays a key role in hepatocellular carcinoma cells in the synergistic antiproliferative effect by 5-fluorouracil and interferon-α. *Int. J. Oncol.* 2006;29:1469–1478.

Address reprint requests or correspondence to:
Dr. Hirohisa Yano
Department of Pathology
Kurume University School of Medicine
67 Asahi-machi
Kurume
Fukuoka 830-0011
Japan

Tel: +81-942-31-7546
Fax: +81-942-32-0905
E-mail: hiroyano@med.kurume-u.ac.jp

Received 23 December 2006/Accepted 11 January 2007

Alteration of dihydropyrimidine dehydrogenase expression by IFN-α affects the antiproliferative effects of 5-fluorouracil in human hepatocellular carcinoma cells

Shinji Oie,[1,3] Mayumi Ono,[1,2,6] Hiroto Fukushima,[3] Fumihito Hosoi,[1,4,5] Hirohisa Yano,[5,6] Yuichiro Maruyama,[1,5] Masamichi Kojiro,[5,6] Tadafumi Terada,[4] Kazuyuki Hirano,[7] Michihiko Kuwano,[1,5] and Yuji Yamada[1,4,5]

[1]Station-II for Collaborative Research and [2]Department of Pharmaceutical Oncology, Graduate School of Pharmaceutical Sciences, Kyushu University, Fukuoka, Japan; [3]Personalized Medicine Research Laboratory and [4]Drug Discovery Laboratory, Taiho Pharmaceutical Co. Ltd., Tokushima, Japan; [5]Research Center for Innovative Cancer Therapy and [6]Department of Pathology, Kurume University School of Medicine, Kurume, Japan; and [7]Laboratory of Pharmaceutics, Gifu Pharmaceutical University, Gifu, Japan

Abstract

Dihydropyrimidine dehydrogenase (DPD) is the rate-limiting enzyme in the catabolism of 5-fluorouracil (5-FU) and its activity is closely associated with cellular sensitivity to 5-FU. This study examines the role of DPD in the antiproliferative effects of 5-FU combined with IFN-α on hepatocellular carcinoma (HCC) cells in culture and asks whether IFN-α could affect DPD expression. The combined action of IFN-α and 5-FU on three HCC lines was quantified by a combination index method. Coadministration of IFN-α and 5-FU showed synergistic effects against HAK-1A and KYN-2 but antagonistic effects against KYN-3. The cellular expression levels of DPD mRNA and protein were markedly up-regulated in KYN-3 cells by IFN-α but were down-regulated in HAK-1A and KYN-2. The expression of thymidylate synthase mRNA and protein was down-regulated by IFN-α in all three cell lines. Coadministration of a selective DPD inhibitor, 5-chloro-2,4-dihydroxypyridine (CDHP), enhanced the antiproliferative effect of 5-FU and IFN-α on KYN-3 ~4-fold. However, the synergistic effects of 5-FU and IFN-α on HAK-1A and KYN-2 were not affected by CDHP. The antiproliferative effect of 5-FU could thus be modulated by IFN-α, possibly through DPD expression, in HCC cells. Inhibition of DPD activity by CDHP may enhance the efficacy of IFN-α and 5-FU combination therapy in patients with HCC showing resistance to this therapy. [Mol Cancer Ther 2007;6(8):2310–8]

Introduction

5-Fluorouracil (5-FU) is widely used in the treatment of various gastrointestinal cancers and other types of tumor. It is converted to the active metabolite 5-fluoro-2′-deoxyuridine-5′-monophosphate (FdUMP) and inhibits thymidylate synthase (TS) activity competitively through the formation of a ternary complex of FdUMP, TS, and 5,10-methylenetetrahydrofolate. Cancer cells with high levels of FdUMP and low levels of TS are thus known to be sensitive to 5-FU (1).

Dihydropyrimidine dehydrogenase (DPD) is a rate-limiting enzyme involved in the degradation of pyrimidine bases and pyrimidine-based antimetabolites, such as 5-FU, and so diminishes the antitumor activity of 5-FU. This catabolism occurs mainly in the liver. DPD activity shows wide variation in both cancer patients and the healthy population (2).

The human DPD gene (*DPYD*) is located on chromosome 1p22. It is a single copy 950-kb gene comprising 23 exons (3), in which 39 mutations and polymorphisms have been identified (4–6). Abnormalities of *DPYD* that decrease DPD activity are observed in 3% to 5% of the total population (7), and several patients with congenital DPD deficiency were reported as suffering from severe toxicity after the administration of 5-FU (8). DPD activity in tumor cells is critical to the antitumor effects of 5-FU (9), and its inhibition is expected to enhance these effects.

Hepatocellular carcinoma (HCC) is the fifth most common malignancy in the world. The most effective treatment for patients with HCC is the surgical resection of hepatic lesions. Local therapeutic approaches, such as transcatheter arterial embolization (10), percutaneous transhepatic ethanol injection (11), microwave coagulation (12), and radiofrequency ablation (13), are also effective. However, these therapies are not sufficient for patients with advanced HCC, for whom surgery is often not suitable and whose 5-year survival rate is extremely low (14). For patients with advanced HCC, the clinical response of

Received 5/15/06; revised 4/22/07; accepted 6/12/07.

Grant support: Health and Labour Sciences Research grants of Third Term Comprehensive Control Research for Cancer from the Ministry of Health, Labour and Welfare, Japan and the 21st Century COE Program for Medical Sciences, Kurume University, supported by the Ministry of Education, Culture, Sports, Science and Technology, Japan.

The costs of publication of this article were defrayed in part by the payment of page charges. This article must therefore be hereby marked *advertisement* in accordance with 18 U.S.C. Section 1734 solely to indicate this fact.

Requests for reprints: Shinji Oie, Station-II for Collaborative Research, Kyushu University, 3-1-1 Maidashi, Higashi-ku, Fukuoka, Japan 812-8582. Phone: 81-92-642-6295; Fax: 81-92-642-6295. E-mail: oh9906ie@qa2.so-net.ne.jp

doi:10.1158/1535-7163.MCT-06-0281

almost every anticancer drug is insufficient, and several combination chemotherapies have been tried. Combined chemotherapy with 5-FU and IFN-α has been used previously for patients with advanced HCC, with improved therapeutic effects (15–17). However, these reports of positive effects are contradicted by a previously observed lack of antitumor activity accompanied by increased toxicity (18). To improve the therapeutic index of 5-FU and IFN-α combination therapy, it is therefore important to establish the cause of this occasional decrease in efficacy and increase in side effects.

Plausible mechanisms, such as an increase in FdUMP, TS inhibition rate, and thymidine phosphorylase activity, a decrease in TS levels, and altered 5-FU pharmacokinetics, have been suggested to explain the improved therapeutic effects of IFN-α and 5-FU (19–23). Takaoka et al. (24) showed that transcription of the *p53* gene is induced by IFN-α/IFN-β, accompanied by an increase in p53 protein level, and that the apoptotic response by IFN-β combined with 5-FU was enhanced. Milano et al. (25) reported that IFN-α inhibits DPD activity in human tumor cells, suggesting that inhibition of DPD activity could be involved in 5-FU–induced antiproliferative activity. Consensus IFN was shown to enhance the antiproliferative effect of 5-FU against hepatoma cells through down-regulation of DPD expression (23). By contrast, increased expression of DPD protein by IFN-γ was reportedly observed at a concentration equivalent to that in the sera of patients (26).

According to the presence or absence of synergism by the combination of 5-FU and IFN-α, we classified six human HCC cell lines into two groups: the S-group containing three cell lines, which showed a synergistic effect, and the A-group containing the remaining three cell lines, which showed additive effects (27). The expression levels of type I IFN receptor subunits were specifically up-regulated by 5-FU in all three cell lines of the S-group but not in those of the A-group (27). In this study, we asked whether DPD could limit the antiproliferative effect of 5-FU against HCC cells in culture when 5-FU was applied in combination with IFN-α. This work also shows that inhibiting DPD activity in HCC cells with high DPD levels improves the efficacy of 5-FU combined with IFN-α, following up-regulation by IFN-α.

Materials and Methods

Drugs

5-FU was purchased from Kyowa Hakko Kogyo Co. Ltd. (5-FU Injection 250 Kyowa) and natural human IFN-α was purchased from Otsuka Pharmaceutical Co. Ltd. (OIF). 5-Chloro-2,4-dihydroxypyridine (CDHP) was a gift from Taiho Pharmaceutical Co. Ltd.

Cell Lines

HCC cell lines, KYN-2, KYN-3, and HAK-1A (28, 29), were grown in DMEM (Nissui Seiyaku Co.) with 10% fetal bovine serum (FetalClone III, Hyclone) in a humidified atmosphere of 5% CO_2 at 37°C. We confirmed the expression of type I IFN receptor subunits 1 and 2 in these three HCC cell lines (27).

Cytotoxicity Tests

Cells were seeded into 96-well plates at 1,000 cells/100 μL/well and incubated overnight. On the following day, 100-μL aliquots containing IFN-α and/or 5-FU with or without CDHP were added to each well and cells were cultured for a further 5 days. The number of viable cells was estimated by assaying the activity of cellular succinate dehydrogenases using WST-8 reagent (Cell Counting Kit-8, Dojindo; ref. 30). We confirmed that untreated groups of KYN-2, KYN-3, and HAK-1A cells grew exponentially for 6 days under these experimental conditions (data not shown).

Combination Index Analysis

The combined effects of 5-FU and IFN-α were quantified using a combination index (CI) method developed by Chou and Talalay (31). This method involves plotting dose-effect curves, for each agent and their combination, using the median-effect equation: $fa / fu = (D / Dm)^m$, where D is the dose of the drug, Dm is the dose required for a 50% effect (equivalent to IC_{50}), fa and fu are the affected and unaffected fractions, respectively ($fa = 1 - fu$), and m is the exponent signifying the sigmoidicity of the dose-effect curve.

In this study, relative concentrations (RC) of IFN-α and 5-FU, determined as (concentration) / (IC_{50} value), were used for analysis. The computer software Xlfit version 2.0.6 (ID Business Solutions Ltd.) was used to calculate the values of Dm and m. The CI used for the analysis of the drug combinations was determined by the isobologram equation for mutually nonexclusive drugs that have different modes of action: $CI = (D)_1 / (Dx)_1 + (D)_2 / (Dx)_2 + (D)_1(D)_2 / (Dx)_1(Dx)_2$, where $(D)_1$ and $(D)_2$ are RCs of drugs 1 and 2 and x is the percentage of inhibition. Combination indices $CI < 1$, $CI = 1$, and $CI > 1$ indicate synergism, additive effects, and antagonism, respectively.

Quantitative Real-time Reverse Transcription-PCR

Total RNA was extracted using Isogen (Nippon Gene Co., Ltd.) and reverse transcribed using a reverse-transcription system (Promega Corp.) according to the manufacturer's instructions. Quantitative real-time reverse transcription-PCR was done with an ABI Prism 7300 (PE Applied Biosystems). The primers used were as follows: TS 5′-GAATCACATCGAGCCACTGAAA-3′ (forward primer), 5′-CAGCCCAACCCCTAAAGACTGA-3′ (reverse primer), and 5′-(FAM)TTCAGCTTCAGCGAGAACCCAGA(TAMRA)-3′ (probe) and DPD 5′-AATGATTCGAAGAGCTTTTGAAGC-3′ (forward primer), 5′-GTTCCCCGGATGATTCTGG-3′ (reverse primer), and 5′-(FAM)TGCCCTCACCAAAACTTTCTCTCTTGATAAGGA(TAMRA)-3′ (probe). Primers and Taqman probes for glyceraldehyde-3-phosphate dehydrogenase were prepared by Assay-on-Demand Gene Expression Products (PE Applied Biosystems).

Western Blotting

HCC cells were cultured for 48 h with 0, 20, 100, or 500 IU/mL IFN-α. Total protein was extracted using a protein extraction reagent (M-PER, Pierce) supplemented with protease inhibitors (Halt Protease Inhibitor

Cocktail kit, Pierce). Cell lysates were loaded into 7.5% SDS-polyacrylamide gels. After electrophoresis, the separated proteins were electrotransblotted onto polyvinylidene difluoride membranes (Immobilon-P membrane, Millipore). After blocking, membranes were probed with antihuman DPD polyclonal rabbit antibody and antihuman TS monoclonal mouse antibody (gifts from Taiho Pharmaceutical). The proteins were visualized using horseradish peroxidase–conjugated antibodies (Pierce) followed by enhanced chemiluminescence (Pierce). The intensity of luminescence was quantified using an image analysis system (LAS-1000, Fuji Film).

Enzyme Assay for DPD Activity

DPD activity was measured using [6-^{14}C]5-FU as a substrate (32, 33). Cells were homogenized and centrifuged at 105,000 × *g* for 60 min at 4°C, and the supernatant was used for assay. A reaction mixture containing 10 mmol/L potassium phosphate (pH 8.0), 0.5 mmol/L EDTA, 0.5 mmol/L 2-mercaptoethanol, 2 mmol/L DTT, 5 mmol/L $MgCl_2$, 20 μmol/L [6-^{14}C]5-FU, 0.1 mmol/L NADPH, and 25 μL of cell extract in a total volume of 50 μL was incubated at 37°C for 30 min. After chemical hydrolyzation and neutralization using KOH and $HClO_4$, a 5-μL aliquot was applied to a TLC plate (2.5 × 20 cm, silica gel 60 F_{254} plate, Merck) and developed with a mixture of ethanol and 1 mol/L ammonium acetate (5:1, v/v) and diethylether, acetone, chloroform, and water (50:50:40:1, v/v). DPD activity was determined as the sum of the products converted from 5-FU (i.e., dihydrouracil, 2-fluoro-β-ureidopropionic acid, and 2-fluoro-β-alanine) that were visualized and quantified with an imaging analyzer (BAS-2000, Fujix).

Results

Comparison of Drug Sensitivity and mRNA Levels of DPD and TS in Three HCC Cell Lines

The sensitivities of three HCC lines, HAK-1A, KYN-2, and KYN-3, to separately administered 5-FU and IFN-α were determined as IC_{50} values. KYN-3 was the most resistant to 5-FU of the three HCC lines. The IC_{50} values of IFN-α in HAK-1A, KYN-2, and KYN-3 cells were 720, 510, and 24 IU/mL, respectively. KYN-3 cellular sensitivity to IFN-α was therefore approximately 30-fold and 20-fold higher than in HAK-1A and KYN-2 cell lines, respectively. The IC_{50} value of IFN-α in HepG2 cells established from human hepatoblastoma and widely used in experiments was found to be over 10,000 IU/mL (data not shown).

Sensitivity was then compared with mRNA levels of DPD and TS, and DPD activity (as conversion rate from [6-^{14}C]5-FU to its metabolites) in the three cell lines, which were shown to be broadly comparable (Table 1). DPD mRNA levels relative to those of KYN-3 cells, taken as 100%, and those of TS relative to HAK-1A, taken as 100%, are shown in Table 1. The cellular level of TS mRNA in KYN-2 cells was much lower than in the other two lines. Basal DPD activity in KYN-3 cells was approximately 5.5-fold and 9.1-fold higher than in HAK-1A and KYN-2 cell lines, respectively.

Quantitative Analysis of the Combination Effects of 5-FU and IFN-α

Dose-response curves of 5-FU alone and in combination with various concentrations of IFN-α are shown in Fig. 1A to C. Because sensitivities to IFN-α and 5-FU alone were different for each HCC cell line, RCs to the IC_{50} value were used. As the concentration of combined IFN-α was increased, the dose-response curves of 5-FU were shifted down in an IFN-α concentration-dependent manner in all three HCC cell lines. For instance, following cotreatment with 312 IU/mL (RC = 0.45) IFN-α,the dose-response curve of HAK-1A to 5-FU was significantly shifted down and the 5-FU IC_{50} value of 2.3 μmol/L was reduced to 0.28 μmol/L. However, there were clear differences between the three HCC cell lines. For KYN-3 cells, after treatment with the equivalent RC, 0.42 (8.0 IU/mL) IFN-α,the dose-response curve of 5-FU was significantly shifted down, but the 5-FU IC_{50} value of 9.6 μmol/L was only reduced to 5.5 μmol/L.

An enhancement factor (EF) was defined to evaluate synergism between 5-FU and IFN-α, based on a 50% antiproliferative effect, as EF = 1 / [(RC of IFN-α) + (RC of 5-FU)]. When EF is 1, this combined effect is additive; values >1 or <1 imply synergistic or antagonistic effects, respectively. EF values of HAK-1A and KYN-2 were >1 at almost all combined doses, but EF values of KYN-3 at all tested combined doses were closer to 1. The combined effect of 5-FU and IFN-α on HAK-1A and KYN-2 cells was thus judged to be synergistic and that on KYN-3 to be additive, consistent with our previous study (27).

Table 1. HCC cell sensitivities to 5-FU and IFN-α, DPD, and TS mRNA expression levels and DPD activities

Cell line	IC_{50}*		Relative mRNA levels†		DPD activity‡ (pmol/min/mg protein)
	5-FU (μmol/L)	IFN-α (IU/mL)	DPD	TS	
HAK-1A	2.1	720	15	100	2.8 ± 0.9
KYN-2	1.8	510	23	14	1.7 ± 0.7
KYN-3	9.8	24	100	46	15.5 ± 1.6

*The IC_{50} value that caused 50% growth inhibition was calculated from the log-logit regression line. The assays were carried out in quadruplicate. Experiments were repeated twice with essentially similar results.

† DPD mRNA levels are shown relative to those of KYN-3 cells, taken as 100%, and TS mRNA levels are shown relative to those of HAK-1A cells, taken as 100%.

‡ Determinations were carried out in triplicate and data represent mean ± SD.